# Optimizing Bispecific Antibody Pretargeting for Use in Radioimmunotherapy[1]

**Robert M. Sharkey,[2] Habibe Karacay, Heidi Richel, William J. McBride, Edmund A. Rossi, Ken Chang, Dion Yeldell, Gary L. Griffiths, Hans J. Hansen, and David M. Goldenberg**

Center for Molecular Medicine and Immunology, Belleville, New Jersey 07109 [R. M. S., H. K., H. R., D. Y., D. M. G.]; IBC Pharmaceuticals, Inc., Morris Plains, New Jersey 07950 [E. A. R., K. C., D. M. G.]; and Immunomedics, Inc., Morris Plains, New Jersey 07950 [W. J. M., G. L. G., H. J. H., D. M. G.]

## Abstract

***Purpose:*** **With increasing interest in pretargeting procedures for improving the delivery of radionuclides for cancer imaging and therapy, this investigation was undertaken to examine how to optimize a bispecific monoclonal antibody (bsMAb) pretargeting procedure for therapeutic applications.**

***Experimental Design:*** **The model system examined was a bsMAb composed of two Fab′ fragments, one from a humanized anti-carcinoembryonic antigen antibody (hMN-14), and the other a murine antibody (679) against histamine-succinyl-glycine. These Fab′ fragments were chemically conjugated to form a $F(ab')_2$ that is joined by a stable thioether bond. The peptide used for these studies (IMP-241) contained two histamine-succinyl-glycine moieties for binding to the 679 portion of the bsMAb and a single 1,4,7,10-tetra-azacyclododecane *N,N′,N″,N‴*-tetraacetic acid chelate for radiolabeling with $^{111}$In.**

***Results:*** **The bsMAb cleared rapidly in nude mice bearing the GW-39 human colonic cancer xenograft. Administration of a radiolabeled peptide 1 day after the bsMAb, using a bsMAb/peptide mole injection ratio of 10:1, allowed for higher tumor accretion than if delayed by 2 days. Tumor uptake measured 3 h after the peptide injection given 1 day after the bsMAb was 11.3 ± 2.2% percentage of injected dose/gram (%ID/g), with just 2.9 ± 0.4% ID/g of the bsMAb in the tumor at this time. Tumor/blood ratios were 8.1 ± 2.1. Peptide uptake was highest in the kidneys, but even so, the tumor/kidney ratio was 2.5 ± 1.9 just 3 h after the peptide injection. Although low bsMAb/peptide mole injection ratios allow for greater concentrations of the peptide in the tumor, kidney uptake is increased at a proportionally higher amount than in the tumor. Therefore, a bsMAb/peptide injection ratio of 10:1 with a 24-h interval was preferred for pretargeting. Increasing the bsMAb dose, and thereby increasing the bsMAb/peptide injection ratio, further enhanced the delivery of the radiolabeled peptide to the tumor, but the interval spacing between the bsMAb and peptide had to be increased. Despite having a lower %ID/g of the bsMAb in the tumor, with a bsMAb/peptide injection ratio of 50:1 and a 48-h interval, tumor uptake of the $^{111}$In-peptide was nearly 30% ID/g, a 1.6-fold improvement over that seen with the 10:1/24-h interval pretargeting group, and tumor/blood was 35:1, and tumor/kidney ratio was 8:1. Two fractionation strategies were also examined. Giving two equal fractions of peptide after a single injection of bsMAb loaded more moles of peptide into the tumor but would not permit higher radioactivity delivery than what could be achieved with a single injection. However, area under the curve analysis indicated that giving repeated cycles of the bsMAb followed by the peptide would enable improvements in the amount of radioactivity delivered to the tumor without increasing the amount delivered to normal tissues, but the timing of the bsMAb/peptide cycles was important to optimize this process. Finally, it was noted that larger tumors (*e.g.* those > 0.3 g) were more likely to have higher peptide uptake in a pretargeting procedure than smaller tumors (*e.g.,* those of ~0.1 g), perhaps due to the greater mass of the bsMAb localized in the larger tumors, but also possibly because of better blood supply in these tumors.**

***Conclusions:*** **These studies reveal principles that might be applied generally to other pretargeting procedures and demonstrate how a bsMAb pretargeting method could potentially exceed a directly radiolabeled antibody in its ability to deliver radionuclides for cancer therapy.**

## Introduction

Targeted cancer therapy is a concept that encompasses a wide range of strategies. One of the earliest, basic targeting approaches comprised the selective delivery of radioactivity to tumors by coupling the radionuclides directly to antibodies generated against antigens expressed by tumor cells (1). Twenty-five years after the initial laboratory studies were performed with animal tumor antigens, the first proof that radiolabeled antibodies could selectively target a human tumor was obtained first in hamsters followed by nude mice (2–4) bearing human tumor xenografts expressing CEA.[3] Several years later, clinical

[1] Presented at the "Ninth Conference on Cancer Therapy with Antibodies and Immunoconjugates," October 24–26, 2002, Princeton, NJ. This work was supported in part by Department of Energy Grant DE-FG01-00NE22941 and Grant 02-1105-CMM-NO from the New Jersey Commission on Cancer Research.

[2] To whom requests for reprints should be addressed, at Center for Molecular Medicine and Immunology, 520 Belleville Avenue, Belleville, NJ 07109. Phone: (973) 844-7000; Fax: (973) 844-7020; E-mail: rmsharkey@gscancer.org.

[3] The abbreviations used are: CEA, carcinoembryonic antigen; AUC, area under the curve; bsMAb, bispecific monoclonal antibody; DOTA, 1,4,7,10-tetra-azacyclododecane *N,N′,N″,N‴*-tetraacetic acid; DTPA,

imaging studies confirmed the feasibility of this approach (5). Although the first studies with radiolabeled antibodies for therapy, termed radioimmunotherapy (6), also were demonstrated in CEA-producing xenografts (7), ultimately the successful application of this technology has come to fruition in hematological tumors, so that now, 25 years after the first clinical demonstration of antibody targeting with anti-CEA antibodies, the first radiolabeled antibody has been approved for NHL therapy (8). Thus, although it has taken many years for this technology to enter the armamentarium of tumor therapy modalities, it is encouraging that there are a number of other radiolabeled antibody-targeting strategies in various stages of development that could also ultimately find acceptance for the use of this treatment method in other cancer types.

Pretargeting, where the therapeutic is decoupled from the targeting agent, is an example of one of these promising new strategies (9). Reardan *et al.* (10) first proposed pretargeting nearly 20 years ago. At that time, the investigators envisioned antibodies with dual specificity, one for a tumor antigen and the other for a hapten. Shortly after this report, Hnatowich *et al.* (11) introduced the idea of using streptavidin or avidin along with biotin as an antibody pretargeting strategy. This novel concept was intriguing because of avidin/biotin's innate high affinity and four binding sites. Several configurations of this pretargeting strategy were possible, but ultimately two procedures dominated. Paganelli and co-workers (12, 13) focused on a method that has evolved to include a targeting step with a biotinylated antibody, followed by a chase and bridging step using a combination of streptavidin and avidin, followed by radiolabeled biotin. This three-step approach has been used clinically and has resulted in promising responses, especially in malignant gliomas (13). Axworthy *et al.* (14, 15) pursued a different method that relied on the pretargeting of streptavidin-conjugated antibody, a clearing/blocking step, followed by the delivery of radiolabeled biotin. Importantly, this group was the first to show that this pretargeting method could be optimized so that a small, rapidly clearing molecule (radiolabeled biotin) could achieve concentrations in a tumor similar to those possible with a radiolabeled IgG, except that the T/NT ratios far exceeded that of the IgG (14). This pretargeting strategy was shown in a human solid tumor xenograft model to be more therapeutically effective than a directly radiolabeled antibody (15), and recently, Press *et al.* (16) extended this finding to a human lymphoma xenograft model. Clinical studies using this approach confirmed excellent targeting ratios (17–19). In Phase I/II therapy trials in colorectal cancer, patients tolerated up to 100 mCi/m$^2$ of $^{90}$Y-biotin before dose-limiting gastrointestinal toxicity was encountered (19). This toxicity was likely due at least in part to gastrointestinal targeting of the primary antibody, NR-LU-10. However, there were also indications of renal toxicity that was manifested >6 months after treatment, which may have been the consequence of primary renal excretion of the $^{90}$Y-biotin (17, 19), but hematological toxicity was not dose-limiting. More recently, Weiden and Breitz (20) reported the use of this pretargeting approach in NHL, using a chimeric anti-CD20-streptavidin-conjugated antibody as the primary targeting agent. Doses of up to 50 mCi/m$^2$ were tolerated with no more than grade 3 hematological toxicity, with radiation doses to the tumor averaging about 30 cGy/mCi. Three complete responses and one partial response were observed in the seven patients treated at the highest dose level.

Another promising pretargeting method uses a bsMAb as the primary targeting agent. Although Reardan *et al.* (10) first described this concept, another group of investigators advanced this technology by showing how a divalent hapten enhances the targeting of a radiolabeled peptide (21), and this principle became known as the "affinity enhancement system." After initially working *in vitro* and *in vivo* with several primary targeting systems to optimize T/NT ratios, Le Doussal *et al.* (22) ultimately focused on the use of a bispecific antibody composed of 2 Fab′ fragments, one against CEA, and the other against indium-loaded DTPA, which were chemically conjugated to form a stable F(ab′)$_2$ fragment. Early clinical testing determined that a minimum dose of 0.1 mg/kg of the bsMAb was required for optimal targeting, using a 4–5-day interval and a hapten dose of 0.1 nmol/kg (22). Gautherot *et al.* (23) subsequently examined the possibility of using this pretargeting approach for therapy with a $^{131}$I-hapten, and by modifying the bsMAb dose, timing, and hapten dose, optimal conditions were derived. They observed that for a fixed amount of bsMAb, if the amount of peptide was increased, progressively more hapten could be bound in the tumor, and for this reason they elected to use a hapten to bsMAb mole ratio of 0.5 (ratio based on the amount of each agent administered). Furthermore, dosimetry studies based on the injection of either 100 μg (1 nmol) or 500 μg (5 nmol) of bsMAb given at 20 or 48 h before either 0.5 or 2.5 nmol of peptide (hapten/bsMAb ratio fixed at 0.5), respectively, showed that the higher protein dose increased the radiation-absorbed dose to the tumor for the pretargeting procedure to a level comparable with that seen with an $^{131}$I-IgG, but with better T/NT ratios. Subsequently, therapy studies in human tumor xenograft models for colorectal and medullary thyroid cancers, using 200–300 μg of the bsMAb followed 24–48 h later with ~1.0–3.0 mCi of the $^{131}$I-hapten (a hapten/bsMAb ratio of 0.5 was maintained), were undertaken (24, 25).

We have investigated both the streptavidin/biotin pretargeting method using a streptavidin-anti-CEA IgG, a clearing agent, and radiolabeled biotin (26, 27) and a bsMAb procedure using a bsMAb composed of an anti-CEA Fab′ together with Fab′ directed against indium-loaded DTPA (28) or against a novel hapten, HSG (29). We elected to focus on the bsMAb approach for pretargeting because this procedure does not rely on the use of an immunogenic substance, streptavidin or avidin. Bispecific antibodies can be developed that are fully humanized, and therefore they should be far less immunogenic than an antibody conjugate or a recombinant protein containing streptavidin or avidin. Indeed, immune responses to streptavidin were observed in 6 of 10 NHL patients who received the chimeric anti-CD20-streptavidin conjugate (20). Although the antibody response was transient and did not prevent retreatment, it does illustrate the immunogenicity of this type of construct, even in a patient population known to have a low incidence of antibody

diethylenetriaminepentaacetic acid; HSG, histamine-succinyl-glycine; MTD, maximum tolerated dose; NHL, non-Hodgkin's lymphoma; %ID/g, percentage of injected dose/gram; HPLC, high pressure liquid chromatography; T/NT, tumor/nontumor.

responses to murine IgG (30, 31). Another possible advantage for the bsMAb approach is that it has been used without an additional step to clear or block the primary targeting antibody before the addition of the radiolabeled peptide (22, 32).

With some very promising possibilities for bsMAb pretargeting, it is important to review the parameters that influence optimization of this procedure. In this article, we provide an overview of a pretargeting system to illustrate factors that contribute to the optimization of this type of pretargeting method, but it is likely that the principles discussed with this system will be applicable to other pretargeting methods as well.

## Materials and Methods

**Preparation of the bsMAb and Peptide.** The bsMAb was composed of a single Fab′ fragment of a humanized anti-CEA antibody, hMN-14 (33), chemically coupled to a single Fab′ fragment of an antibody to HSG, designated m679 (34). The conjugation procedure was described previously (29) and involves the use of *N,N′*-1,2-phenylenedimaleimide (Aldrich Chemical Co., Milwaukee, WI), a bifunctional coupling agent that creates a stable thioether linkage between the two Fab′ fragments using the free sulfhydryl groups formed on the Fab′ after reduction of the parental $F(ab')_2$ fragments (35). The resulting bsMAb will have the two Fab′ fragments properly oriented to form a $F(ab')_2$ fragment that will not dissociate in serum (28). By carefully controlling this reaction, reformation of the monospecific antibody is minimized, and yields of purified bsMAb $F(ab')_2$ can be expected to be 35–45%. Purification by size-exclusion chromatography is typically all that is necessary to isolate the $F(ab')_2$ from unreacted Fab′. Size-exclusion HPLC of the purified products has shown a single peak. SDS-PAGE was performed on each lot of bsMAb prepared, using 2.5-μg aliquots of each. They were loaded onto Bio-Rad 4–20% (Tris-HCl) linear gradient precast electrophoresis gels (8.6 cm × 6.8 cm × 1.0 mm). Samples were prepared by diluting solutions of 1 μg/μl at 1:1 with reducing and nonreducing buffers. The sample buffer contained 0.01 M Tris-HCl, 2.0% SDS, 15 sucrose (w/v), and 0.01% bromphenol blue (pH 7.2). For reducing conditions, DTT was added to the sample buffer to 12 mg/ml, and for nonreducing conditions, iodoacetamide was added to sample buffer to14 mg/ml before diluting the samples 1:1. These solutions were heated for 20 min at 60°C and then cooled in an ice bath before loading on the gel. The running buffer was 0.025 M Tris, 0.1 M glycine, and 0.1% SDS (pH 8.5). Under reducing conditions, these conjugates had a molecular weight of approximately 100,000, and thus this was used for all determinations of molar concentration of the bsMAb.

The peptide used for these studies is designated IMP-241. It is composed of four amino acids, a single DOTA for binding radiometals, and two HSG groups for binding to the 679 antibody [DOTA-Phe-Lys(HSG)-Tyr-Lys(HSG); $MH^+$ by mass spectroscopy is 1471]. The synthesis of this peptide was described previously (29).

**Radiolabeling.** The bsMAb was radioiodinated with $Na^{125}I$ (Perkin-Elmer, Boston, MA) using the chloramine-T method (36) to a specific activity of between 10 and 15 mCi/mg. $^{111}InCl_3$ was purchased from IsoTex (Friendsville, TX) in 0.05 M HCl at >200 mCi/ml. Peptide IMP-241 was dissolved in 0.5 M ammonium acetate (pH 5.5) at $2.2 \times 10^{-3}$ M concentration and stored frozen at −20°C. For labeling, to 3 mCi of $^{111}InCl_3$, 0.5 M ammonium acetate (pH 4.0) was added at 3× the volume of $^{111}InCl_3$. After adding 2.32 μl of IMP-241 ($5.10 \times 10^{-8}$ mol), the mixture was centrifuged and heated in a lead pig for 30 min in a boiling water bath. The mixture was cooled on ice for 5 min and centrifuged again. DTPA (0.1 M) was added to a final concentration of 3 mM. After 15 min at room temperature, 0.1 M sodium acetate (pH 6.5) was added to raise the volume to 1 ml. Instant thin-layer chromatography and HPLC analyses of the product were performed. Instant thin-layer chromatography strips were developed in saturated sodium chloride. Reverse-phase HPLC analyses were performed on a Waters 8 × 100-mm radial Pak cartridge filled with a C-18 nova-Pak 4 μm stationary phase. The column was eluted at 1.5 ml/min with a linear gradient of 100% A (0.075% trifluoroacetic acid in water) to 55% A and 45% B, where B was 0.075% trifluoroacetic acid in 75% acetonitrile and 25% water, over 15 min. At 15 min, the solvent was switched to 100% B and maintained there for 5 min before re-equilibration to initial conditions. Reverse-phase HPLC analyses showed a single peak at 11.8 min. $^{111}$In-IMP-241 was mixed with excess m679 IgG on a Bio-Sil SE 250 HPLC gel filtration column and showed a peak at the retention time of the antibody, indicating binding to the antibody. The clearance and tumor targeting properties of the $^{111}$In-IMP-241 were reported previously in this human tumor xenograft nude mouse model system (29).

***In Vivo* Biodistribution and Pretargeting Studies.** All studies were performed in female nude mice (6–9-weeks old) bearing s.c. GW-39 human colonic tumor xenografts (37). GW-39 is serially propagated in nude mice by aseptically harvesting 1.0–2.0-g tumors and mincing tumor with scissors followed by passage through wire mesh. The tumor is suspended in saline to give a 10% (w/v) tumor suspension. Mice receive s.c. injection with 0.2 ml of the suspension, and within 2 weeks, tumors are of sufficient size to begin treatment. Tumor sizes and the number of animals used for each study are provided in "Results;" the bsMAb and peptide are injected i.v. at the doses and amounts also indicated in "Results." In each study, a trace amount of the $^{125}$I-bsMAb (5–10 μCi) was added to the total injected dose. Animals were typically received injection with with 8.8 μCi of $^{111}$In-labeled peptide without the addition of unlabeled peptide, whereas in others, unlabeled peptide was added to achieve the desired moles of peptide. In most studies, animals were necropsied 3 and 24 h after the injection of the peptide. Additional time points were examined to derive AUC for the radiolabeled peptide. For fractionated injection schemes, the effective time-activity data of the first and second injections were calculated independently for all injection schemes from the measured biological uptake. If measured uptake data were not available for a particular time, the data were extrapolated using the half-life determined from the previous time points using a monoexponential fit. The total effective activity uptake at each time point was the resulting sum of the activity of first and second fractionated injections. The AUC of all injection schemes was determined by the trapezoidal method to the last measured or extrapolated time point. The AUC after the last time point was calculated from the effective $T_{1/2}$ of all of the time-activity data, starting after the second injection was given.

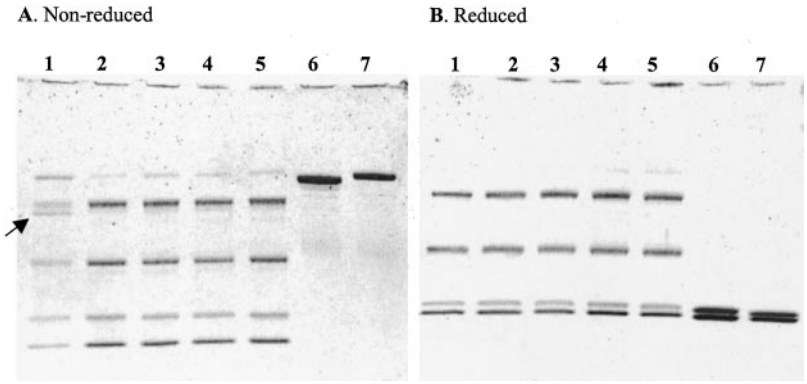


*Fig. 1* SDS-PAGE of different batches of bsMAb (*Lanes 1–5*) and F(ab′)$_2$ fragments of hMN-14 (*Lane 6*) and m679 (*Lane 7*) under non-reducing (*A*) and reducing conditions (*B*).

To maintain consistency, the effective cumulative uptake for all injection schemes was determined up to 240 h after the first injection was administered.

## Results

### *Properties of the bsMAb*

The most convenient bsMAb to prepare is one that is composed of two chemically conjugated Fab′ fragments, with one Fab′ directed to the intended target, whereas the other binds a particular effector molecule. In the system described herein, the primary targeting portion of the bsMAb is to CEA, and the anti-hapten antibody portion of the bsMAb is directed against HSG (34). The conjugation method forms a stable thioether linkage between each of the Fab′ fragments (35). With properly controlled conditions, the Fabs are likely joined by the same sulfhydryl group that linked the two heavy chains of the parental F(ab′)$_2$. SDS-PAGE confirms the stability of the heavy chain linkage because, unlike unconjugated F(ab′)$_2$ fragments, under reducing conditions, a band representing the two heavy chains remains (Fig. 1). The bands seen by SDS-PAGE are similar to those reported by Glennie *et al.* (35) for this type of conjugate and can be useful for discriminating differences between lots of bsMAb. For example, *Lanes 1–5* in Fig. 1 show five lots of bsMAb. During the preparation of one lot of bsMAb (*Lane 1*), the reduction step was mistakenly carried out for a longer duration than intended. Although all other parameters, such as size-exclusion HPLC and immunoreactivity of this lot of antibody, were identical to the others, SDS-PAGE showed an additional band that was not as apparent on the other samples (Fig. 1*A, arrow*). In animals, this bsMAb seemed to clear more quickly than the other lots, resulting in about 2-fold lower bsMAb concentrations in the blood. Although tumor targeting data for pretargeting were unaffected, we elected not to continue use of this lot of antibody to ensure greater consistency among experiments. Because this bsMAb construct is chimeric (*i.e.*, composed of humanized and a murine Fab′), it clears very rapidly from the blood when compared with a bsMAb composed entirely of murine Fab′ (see below). Therefore, it is uncertain whether the full extent of the alteration in biodistribution that might have occurred by over-reducing the antibody could be appreciated, but at least SDS-PAGE analysis provides a means to examine lot-to-lot variations in the quality of a given bsMAb preparation that can then be correlated with *in vivo* behavior.

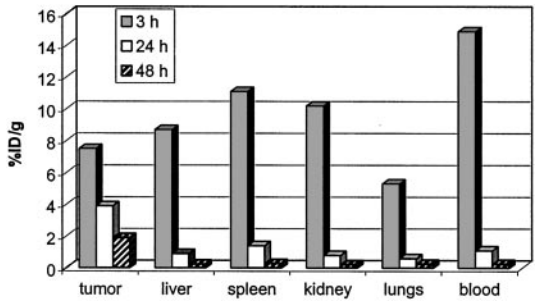


*Fig. 2* Normal tissue distribution of $^{125}$I-hMN-14 × m679 F(ab′)$_2$. Tumor-bearing nude mice ($n$ = 3 for each time interval) were injected with 15 μg of the bsMAb that contained a tracer amount (10 μCi) of the $^{125}$I-bsMAb. Animals were necropsied at the times indicated.

### *Biodistribution of the bsMAb*

Before examining pretargeting, the biodistribution and tumor targeting of the bsMAb must be examined. Fig. 2 illustrates the distribution of the hMN-14 × m679 F(ab′)$_2$ bsMAb in normal tissues. Tumor uptake was highest at the earliest time examined (3 h), with a gradual decrease over time. Uptake in the normal tissue showed a more rapid exponential decrease than that in tumor. As we reported previously (28, 29), these chemical conjugates formed with thioether linkages between the two Fabs are stable in plasma, but this conjugate, like several others we have studied that use a humanized antitumor antibody combined with a murine or chimeric form of the anti-hapten antibody, clears very rapidly from the blood in contrast to a chemically conjugated bsMAb composed entirely of murine Fabs. Depending on the lot of bsMAb and sometimes the shipment of animals used, 1 day after the bsMAb injection, concentrations in the blood typically range from 0.5% to 1.0% ID/g, and concentrations in GW-39 tumors average between 3.0% and 4.0% ID/g. The rapid blood clearance of these chimeric bsMAbs is most likely due to foreign nature of the conjugate because splenic uptake is prominent at early time points, suggesting that the bsMAb is recognized and cleared by the reticuloendothelial system. This rapid blood clearance is an advantage for these models because for pretargeting, a low blood concentration of the bsMAb is essential for optimization of conditions. However, the rapid blood clearance also reduces the percentage of the

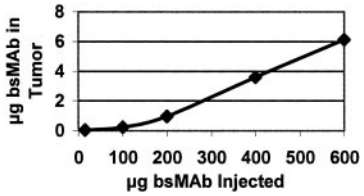


*Fig. 3* The effect of increasing bsMAb protein dose on the amount of bsMAb in GW-39 tumors. Nude mice ($n = 5$ for each dose level) bearing 0.119–0.247-g GW-39 tumors received injection with 15–600 μg of bsMAb, with each dose containing a trace amount of $^{125}$I-bsMAb. Animals were necropsied 24 h later, and based on the amount of $^{125}$I-bsMAb in the tumor, the amount of bsMAb protein (in micrograms) in the tumor was determined. The %ID/g in the tumor (data not shown) was similar among the doses tested, suggesting that there were still additional antigen sites in the tumor available for bsMAb binding.

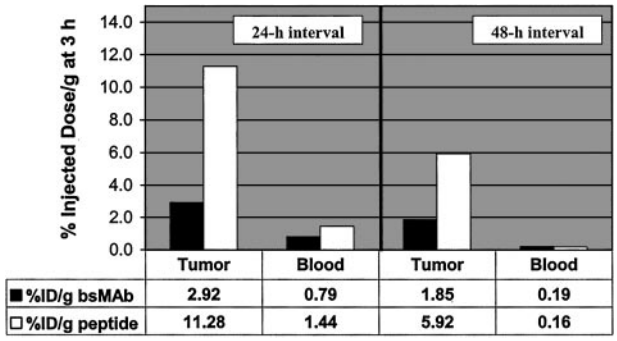


*Fig. 4* Pretargeting of $^{111}$In-IMP-241 (0.015 nmol) with the hMN-14 × m679 F(ab′)$_2$ bsMAb (0.15 nmol containing a trace amount of $^{125}$I-bsMAb) in nude mice bearing GW-39 human colonic cancer xenografts. IMP-241 was injected at either 24 or 48 h after the bsMAb injection. Tumor sizes were 0.25 ± 0.15 and 0.22 ± 0.08 for the 24- and 48-h intervals, respectively ($n = 5$ animals/group).

bsMAb that localizes in the tumor. Therefore, considerably more bsMAb would need to be given to load the antigen sites with this type of bsMAb than would be required if the conjugate cleared more slowly. For example, our prior experience showed that in similarly sized GW-39 tumors, about 400 μg of a radiolabeled murine anti-CEA IgG that clears slowly were required to bind most of the available antigen (38–40). Dose escalation with the hMN-14 × m679 F(ab′)$_2$ bsMAb showed no evidence for saturation of antigen binding sites in GW-39 tumors with as much as 600 μg of the bsMAb (Fig. 3). Using the prior experience with the whole IgG to estimate the number of moles of antibody/gram that can bind to GW-39, it could require as much as 1.6–3.6 mg of bsMAb to saturate CEA in GW-39 tumors. Thus, the amount of bsMAb used for the pretargeting studies reported herein does not approach antigen saturation levels. In addition, over this protein dose range, the bsMAb had essentially the same %ID/g in the normal tissues (most importantly, the blood).

### *Pretargeting*

Optimizing pretargeting is a multistep process that requires examining the interrelationships between the bsMAb dose, the interval between the bsMAb and peptide injection, and the peptide dose. This can be carried out in a number of different ways and could be different for each model system. Nevertheless, the process given below is a reasonably straightforward method that addresses each of the major issues.

**Interval Timing.** One of the first factors to examine is the appropriate interval between the bsMAb and radiolabeled peptide/hapten. If the peptide is injected too soon after the bsMAb is given, a large fraction will bind to the bsMAb in the blood before it has an opportunity to localize to the tumor. However, because the bsMAb concentration in the tumor could also decrease over time, delaying the peptide injection could decrease the availability of bsMAb for capturing the peptide. Interval timing should be conducted first with a fixed amount of bsMAb and peptide, but with the understanding that this interval might require further adjustment if either the bsMAb or peptide dose changes. As long as the bsMAb clearance and distribution are not affected over a wide protein dose range, the administered doses of the bsMAb and peptide can be kept to a minimum for the initial testing. Fig. 4 shows an example of the targeting data obtained using 15 μg (0.15 nmol) of $^{125}$I-bsMAb followed 24 or 48 h later with 0.015 nmol of $^{111}$In-IMP-241 (*i.e.,* a 10:1 bsMAb/peptide mole ratio based on the amount of each agent injected). Three h after the peptide was given, animals were necropsied, and the %ID/g values for the bsMAb and peptide were determined. In the group of animals given the peptide 24 h after the bsMAb and 3 h after the peptide was given, there were 2.9 ± 0.41% ID/g of the bsMAb in the tumor and 0.79 ± 0.24% ID/g in the blood. For the peptide, there were 11.28 ± 2.17% ID/g in the tumor and 1.44 ± 0.33% ID/g in the blood, with tumor/blood ratios of 8.1 ± 2.1. Delaying the peptide injection for 48 h allowed additional time for the bsMAb to clear from the blood, reducing it to 0.19 ± 0.05% ID/g, but the concentration of the bsMAb in the tumor also decreased nearly 2-fold to 1.85 ± 0.84% ID/g. Consequently, the amount of peptide bound to the tumor was also reduced 2-fold to 5.92 ± 2.13% ID/g. However, with only 0.16 ± 0.09% ID/g of the peptide in the blood, nearly 10-fold less than that seen with the 24-h interval spacing, tumor/blood ratios increased to 42.9 ± 20.0.

Because successful therapy requires maximizing the amount of radioactivity delivered to the tumor, and because the 24-h interval delivered nearly twice the amount of peptide to the tumor, this interval would have the advantage of delivering a higher amount of radioactivity to the tumor. It could be argued, however, that because the 48-h spacing had significantly improved tumor/blood ratios, if hematological toxicity was dose-limiting, by using the 48-h spacing, the injected radioactivity dose of the peptide could be increased, perhaps by as much as 10-fold (*i.e.*, to bring it to the same amount as the 24-h interval), thereby compensating for the lower amount in the tumor. However, because the percentage of uptake of the peptide in the kidneys is relatively unaffected by the interval spacing (*e.g.,* at 3 h, 4.61 ± 0.71% and 3.17 ± 0.56% ID/g were in the kidney at the 24- and 48-h intervals, respectively), this approach would appreciably increase the radiation dose to the kidneys. Indeed, the majority of the peptide localized in the kidney can be explained by the peptide's clearance through this organ. For example, in this study, animals given the same dose of the $^{111}$In-IMP-241 alone had 2.1 ± 0.2% ID/g in the kidney

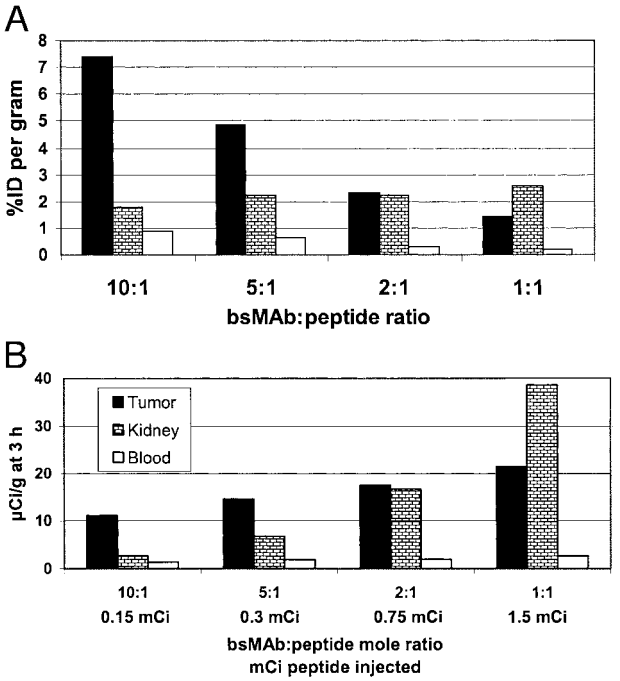


*Fig. 5* The effect of altering the bsMAb/peptide ratio on the biodistribution of the radiolabeled peptide: fixed bsMAb protein dose, increasing peptide. Nude mice bearing GW-39 tumors (0.28–0.36 g) were injected i.v with 0.15 mg (1 nmol) of the hMN-14 × m679 $F(ab')_2$ bsMAb. Twenty-four h later, $^{111}$In-IMP-241 was injected i.v. Additional unlabeled peptide was mixed with the radiolabeled peptide so that the total amount of peptide injected into each group of animals ($n = 5$) would mimic the moles of peptide required for administering 0.15–1.5 mCi of $^{90}$Y-IMP-241. Three h after the peptide injection, animals were necropsied, and the amount of the bsMAb (based on the coinjection of $^{125}$I-bsMAb) and $^{111}$In-peptide was determined in the organs. Shown here is the peptide uptake in the tumor, kidney, and blood. *A,* data are represented as %ID/g (*line interval* = 1.5% ID/g), whereas in *B*, the data represent the amount of radioactivity that would be in the tissue at this time at the dosage of $^{90}$Y-peptide represented. *Symbols* are as defined in *B*.

at 3 h. Therefore, about 50–70% of the peptide in the kidney in the pretargeting animals could be explained by the peptide's clearance and reabsorption in this organ. Liver uptake of the radiolabeled peptide was not an issue with either of these intervals, with tumor/liver ratios exceeding 20:1 and 50:1 for the 24- and 48-h intervals, respectively.

**The bsMAb/Peptide Mole Ratio.** The 24-h interval was determined to be the best interval when the mole ratio of the injected bsMAb and peptide was 10:1. However, pretargeting is also highly dependent on this molar ratio. Several studies were performed to illustrate the critical importance of the bsMAb/peptide mole ratio for optimizing pretargeting. In the first example, a study was designed to show what might occur in a situation where the dose of the radiolabeled peptide was increased (*e.g.,* in determining the radioactivity MTD) without concomitantly increasing the bsMAb dose to maintain the bsMAb/peptide ratio (Fig. 5). Tumor-bearing nude mice received injection with 0.1 mg (1 nmol) of the bsMAb, and 24 h later, increasing moles of $^{111}$In-labeled IMP-241 were injected to simulate the administration of radioactivity doses of 0.15–1.5 mCi of $^{90}$Y-IMP-241 (*i.e.*, 0.1–1.0 nmole). Animals were necropsied 3 h later. The average % ID/g values of the bsMAb in the tumor, kidneys, and blood were not significantly different among the groups, ranging from 3.7% to 4.4% ID/g, 0.5% to 0.7% ID/g, and 0.8% to 0.9% ID/g, respectively, which are similar to the results observed when only 15 μg of bsMAb were given (*i.e.*, Fig. 4). Indeed, the targeting data for both the bsMAb and the peptide in this study using a 10:1 bsMAb/peptide ratio and a 24-h interval were the same as those seen in the previous study, where only 15 μg of bsMAb were injected with the corresponding amount of peptide. This suggests that if the bsMAb/peptide ratio is held constant at a given interval spacing, the targeting data for the peptide could be similar over a given dose range. However, when this ratio is changed, in this case by increasing the peptide dose while the bsMAb dose remains fixed, the % ID/g of the peptide localized to tumor and the normal tissues decreases proportionally, thereby maintaining T/NT ratios. The notable exception is the kidneys (Fig. 5*A*), where the % ID/g remains unchanged, because the renal uptake is related primarily to the peptide's clearance properties. As a consequence, the tumor/blood ratio at the 10:1 ratio was 8.1 ± 1.9 compared with 8.6 ± 1.4 at the 1:1 ratio, but the tumor/kidney ratio decreased from 4.1 ± 1.1 to 0.6 ± 0.06. The impact on the kidneys can perhaps be better appreciated by examining how much $^{90}$Y radioactivity would be delivered under these conditions. As shown in Fig. 5*B*, increasing the amount of peptide increases the amount of radioactivity delivered to the tumor by nearly 2-fold when going from a 10:1 to a 1:1 ratio (*i.e.*, 0.15 to 1.5 mCi). However, the amount of radioactivity delivered to the kidney increases 14-fold over this same range. Blood concentrations also increase from 1.4 to 2.6 μCi, which suggests that as the amount of peptide in the circulation increases, the likelihood that the peptide will bind to circulating bsMAb is increased. Although at a bsMAb/peptide ratio of 5:1 the amount of radiolabeled peptide delivered to the tumor was higher compared with a 10:1 ratio, this increase was hardly substantial (increasing from 11.1 to 14.6 μCi) compared with the kidneys (increasing from 2.7 to 6.8 μCi). Here again, targeting is optimized using the 10:1 ratio at a 24-h interval.

Converting the % ID/g for the bsMAb and the peptide, we see that at the 10:1 bsMAb/peptide ratio, the resulting peptide/bsMAb mole ratio in the tumor at 3 h was 0.16. This increased to 0.29 when the bsMAb/peptide injection ratio was 5:1 and reached 0.39 at a 1:1 ratio. Because not all of the bsMAb was bound by the peptide, further increases in the peptide dose would have likely loaded more peptide in the tumor. However, for affinity enhancement system to aid in stabilization of the peptide in the tumor, this ratio should not exceed 0.5 (*i.e.*, 1 peptide binding across 2 bsMAb). In this regard, it might be possible that by increasing the peptide dose to maximize the loading of the bsMAb, the peptide binding to the tumor could be destabilized. Thus, it is preferable that the mole ratio of the peptide to the bsMAb in the tumor favors the bsMAb.

This study was also performed in a converse manner; namely, the peptide dose was fixed, but the bsMAb dose was increased, and a 24-h interval was maintained. For this study, the amount of peptide administered was fixed at a level sufficient to deliver 1.0 mCi of $^{90}$Y-IMP-241. Animals received

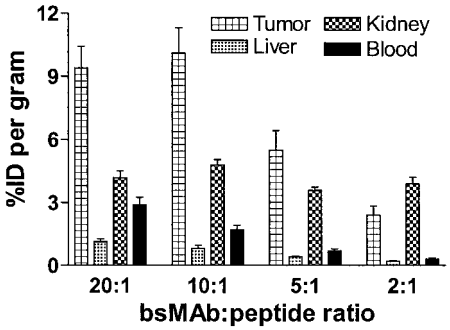


*Fig. 6* The effect of altering the bsMAb/peptide ratio on the biodistribution of the radiolabeled peptide: fixed peptide dose, increasing bsMAb. Tumor-bearing (average, 0.26–0.37 g; $n = 4$–5) nude mice were given increasing amounts of bsMAb starting at 73.2 μg (2:1 ratio) to 732 μg (20:1 ratio), and 24 h later, 0.366 nmol of $^{111}$In-IMP-241 was given. Animals ($n = 5$) were necropsied 3 h after the peptide injection, and the amount of $^{125}$I-bsMAb and $^{111}$In-IMP-241 in the tissues was determined. *Bars* indicate the mean ± SD of the %ID/g in each of the tissues shown.

increasing amounts of the bsMAb starting at 73.2 to 732 μg (0.732–7.32 moles), and 24 h later, the animals were given 0.366 nmol of the peptide radiolabeled with $^{111}$In. Three h later, the animals were necropsied, and the uptake in the tissues was determined. Based on $^{125}$I-bsMAb added to each dose, there were no significant differences in the biodistribution of the bsMAb over the dose range examined. Tumor uptake for the bsMAb averaged between 2.2 and 3.0% ID/g, and the blood averaged between 0.6 and 0.8% ID/g in the four different groups. Fig. 6 shows the tissue distribution of the $^{111}$In-peptide. Because kidney uptake was unaffected by the different dosages given, at a 2:1 bsMAb/peptide injection ratio, tumor/kidney ratios were <1.0. With increasing doses of the bsMAb (*i.e.*, increasing bsMAb/peptide injection mole ratios), the percentage of uptake of the radiolabeled peptide increased in the tumor, and thus tumor/kidney ratios improved from 0.6 ± 0.1 at the 2:1 ratio to 2.1 ± 0.5 at the 10:1 ratio. Although the uptake in the kidney was unchanged, peptide uptake in all of the other normal tissues increased. However, for the most part, the increase in tumor uptake compensated for the increased uptake in normal tissues. For example, tumor/blood ratios were 8.5 ± 0.8 at the 2:1 bsMAb/peptide ratio and 6.8 ± 3.2 at the 10:1 ratio, but at a 20:1 ratio, tumor/blood ratios decreased significantly to 3.4 ± 1.0 ($P = 0.061$, 20:1 *versus* 10:1; $P = 0.034$, 20:1 *versus* 5:1). In addition, there was no further improvement in the peptide uptake in the tumor by increasing the bsMAb from a 10:1 ratio to a 20:1 ratio. This suggests that at a 20:1 ratio, it was beginning to become more favorable for the peptide to bind to the bsMAb in the blood, because even though the %ID/g of the bsMAb in the blood was the same, there were twice as many moles of the bsMAb in the blood at the 20:1 ratio than at the 10:1 ratio. With a higher concentration (*e.g.,* moles/ml) of bsMAb in the blood and with the fixed amount of peptide being given, there is a greater likelihood that the peptide will bind to the bsMAb in the blood. Thus, these studies reaffirmed that a 10:1 bsMAb/peptide injection mole ratio with a 24-h interval provides the highest tumor uptake along with high T/NT ratios.

Because the ratio of the amount of bsMAb and peptide is so critical to defining the targeting of the peptide, it is actually the peptide dose (*i.e.*, the moles of peptide used to deliver radioactivity that will determine the MTD for the radioactivity, or in imaging applications, the amount of radioactivity required to optimize counting statistics) that will define how much bsMAb should be given to optimize a pretargeting procedure. The prevailing wisdom for pretargeting strategies has been to administer as much bsMAb as possible, so that most of the antigen in the tumor will be bound by the primary targeting agent, thereby establishing as many binding sites as possible to capture the peptide when it is administered. This might initiate a process where the highest possible bsMAb dose is first selected, followed by escalating the amount of peptide to determine the MTD at this fixed bsMAb. However, these animal studies suggest that it is important to first establish an appropriate mole relationship between the bsMAb and peptide and an interval spacing that optimizes the targeting parameters at this ratio (*i.e.*, provides high tumor uptake with optimal T/NT ratios). However, there are yet more factors involved.

In this last study, at a 20:1 ratio with the 24-h interval, there was too much bsMAb in the blood to allow for further improvements in the uptake of the peptide in the tumor. To accommodate higher bsMAb doses, the interval would need to be increased. Increasing the interval between the bsMAb and the peptide increases the chances that the amount of bsMAb in the tumor will decrease, and thus there may be no real gain in peptide delivery. This situation was observed with an IgG × Fab′ bsMAb studied by us (41). This bsMAb conjugate had nearly 20% ID/g in the tumor within a few days of its injection, but the concentration of bsMAb in the blood at this time prevented the targeting of the radiolabeled peptide to the tumor (41). To get the concentration of the bsMAb to a low enough level for good peptide targeting, the interval had to be increased to 11 days, at which time the concentration of the bsMAb in the tumor decreased to 3% ID/g. At this time, the pretargeting with an IgG × Fab′ conjugate was no better than the peptide targeting seen when given 2 days after $F(ab')_2$ × Fab′ bsMAb, which had the same %ID/g of bsMAb in the tumor at 2 days as the IgG × Fab′ conjugate had at 11 days. Indeed, the clearance rate of the bsMAb from the blood is a critical factor in optimizing pretargeting and determining whether increasing the protein dose would be beneficial.

**Reassessment of Interval Spacing with Higher bsMAb Dose.** In our model, a 10:1 bsMAb/peptide ratio with a 24-h interval was considered optimal for pretargeting. Increasing the bsMAb dose so that the ratio is 20:1 did not lead to improved peptide targeting because too much bsMAb was in the blood at this time. Thus, the bsMAb concentration in the blood at the 10:1 ratio with a 24-h interval spacing was low enough so that a substantial fraction of the peptide was free to eventually localize in the tumor. If higher bsMAb doses were to be used with a fixed amount of peptide, the issue becomes how long will it take for the blood concentration of a given dose of bsMAb to decrease to the same level as that seen at the 10:1 ratio/24-h interval? Based on 0.8% ID/g of bsMAb in the blood at 24 h, if 1 nmol of bsMAb were injected, there would be 0.008 nmol of bsMAb per gram of blood when 0.1 nmol of peptide was given, which means there were 12.5 moles of peptide injected for every

*Table 1* The effect of increasing the bsMAb protein dose using a fixed amount of radiolabeled peptide

GW-39 tumor-bearing nude mice were given either 50 or 250 μg of bsMAb (0.5 and 3.0 nmol) spiked with $^{125}$I-bsMAb. At either 24 or 48 h after the bsMAb dose, animals were given 0.05 mol of $^{111}$In-IMP-241, which gave the animals either a 10:1 or a 50:1 bsMAb/peptide mole injection ratio (50 and 250 μg of bsMAb, respectively). At 3 and 24 h after the peptide was given, groups of five animals were necropsied, and the distribution of $^{125}$I-bsMAb and $^{111}$In-IMP-241 was determined. Data are presented as the means ± SD for the %ID/g of both the bsMAb and peptide and T/NT ratios for the peptide. Tumor weights are given in parentheses, the first being the average weight in animals necropsied at 3 h and the second being the average weight for 24-h necropsy group.

| | 3 h after $^{111}$In-IMP-241 | | | 24 h after $^{111}$In-IMP-241 | | |
|---|---|---|---|---|---|---|
| | $^{125}$I-bsMAb | $^{111}$In-IMP-241 | | $^{125}$I-bsMAb | $^{111}$In-IMP-241 | |
| | %ID/g | %ID/g | T/NT | %ID/g | %ID/g | T/NT |
| 10:1/24 h | | | | | | |
| Tumor (0.43 ± 0.08) (0.57 ± 0.07) | 3.80 ± 0.73 | 18.39 ± 4.19 | | 2.92 ± 0.61 | 14.21 ± 3.22 | |
| Kidney | 0.43 ± 0.14 | 3.14 ± 0.51 | 5.9 ± 1.6 | 0.16 ± 0.01 | 2.69 ± 0.37 | 5.4 ± 1.2 |
| Liver | 0.55 ± 0.11 | 0.51 ± 0.12 | 38.6 ± 15.8 | 0.22 ± 0.03 | 0.69 ± 0.10 | 20.8 ± 4.5 |
| Lungs | 0.41 ± 0.07 | 0.78 ± 0.09 | 24.0 ± 6.8 | 0.18 ± 0.02 | 0.44 ± 0.12 | 32.3 ± 4.2 |
| Blood | 0.59 ± 0.09 | 1.25 ± 0.25 | 15.7 ± 6.6 | 0.21 ± 0.02 | 0.25 ± 0.03 | 57.6 ± 10.8 |
| 10:1/48 h | | | | | | |
| Tumor (0.56 ± 0.07) (0.46 ± 0.05) | 1.78 ± 0.46 | 9.64 ± 2.67 | | 1.62 ± 0.37 | 7.74 ± 1.67 | |
| Kidney | 0.24 ± 0.03 | 5.86 ± 1.14 | 1.7 ± 0.5 | 0.17 ± 0.16 | 2.45 ± 0.27 | 3.2 ± 0.9 |
| Liver | 0.24 ± 0.02 | 0.23 ± 0.02 | 41.5 ± 9.1 | 0.10 ± 0.02 | 0.13 ± 0.03 | 61.7 ± 15.4 |
| Lungs | 0.20 ± 0.03 | 0.47 ± 0.26 | 20.9 ± 4.5 | 0.08 ± 0.04 | 0.13 ± 0.12 | 82.5 ± 38.5 |
| Blood | 0.26 ± 0.04 | 0.26 ± 0.05 | 38.1 ± 11.1 | 0.09 ± 0.04 | 0.05 ± 0.03 | 165.0 ± 39.4 |
| 50:1/24 h | | | | | | |
| Tumor (0.48 ± 0.04) (0.37 ± 0.09) | 3.68 ± 0.45 | 19.88 ± 5.09 | | 5.33 ± 1.52 | 26.92 ± 10.05 | |
| Kidney | 0.50 ± 0.08 | 5.17 ± 0.46 | 3.9 ± 1.3 | 0.46 ± 0.06 | 4.65 ± 0.52 | 6.6 ± 3.1 |
| Liver | 0.60 ± 0.08 | 3.24 ± 0.76 | 6.5 ± 2.6 | 0.55 ± 0.06 | 2.91 ± 0.73 | 9.8 ± 4.2 |
| Lungs | 0.56 ± 0.06 | 3.83 ± 0.94 | 5.6 ± 2.4 | 0.14 ± 0.03 | 3.81 ± 1.34 | 8.3 ± 5.0 |
| Blood | 0.79 ± 0.10 | 9.45 ± 2.42 | 2.2 ± 0.9 | 0.19 ± 0.03 | 8.97 ± 2.37 | 3.1 ± 1.2 |
| 50:1/48 h | | | | | | |
| Tumor (0.59 ± 0.09) (0.57 ± 0.07) | 2.49 ± 0.34 | 29.17 ± 5.05 | | 1.56 ± 0.27 | 20.33 ± 2.33 | |
| Kidney | 0.22 ± 0.04 | 3.55 ± 0.32 | 8.3 ± 1.9 | 0.11 ± 0.02 | 2.23 ± 0.13 | 9.1 ± 0.9 |
| Liver | 0.16 ± 0.03 | 0.34 ± 0.06 | 85.1 ± 8.3 | 0.11 ± 0.02 | 0.41 ± 0.10 | 51.3 ± 11.3 |
| Lungs | 0.14 ± 0.03 | 0.60 ± 0.21 | 51.6 ± 11.9 | 0.09 ± 0.02 | 0.42 ± 0.11 | 50.6 ± 10.6 |
| Blood | 0.19 ± 0.03 | 0.86 ± 0.23 | 35.2 ± 5.9 | 0.11 ± 0.02 | 0.35 ± 0.11 | 62.7 ± 19.7 |

mole of bsMAb per gram of blood. Thus, if higher bsMAb doses were administered with this fixed amount of peptide, then the interval would need to be increased to a time when the bsMAb concentration in the blood would be 0.008 nmol/g. If, at this new time interval, there were more moles of bsMAb in the tumor than that seen at the 10:1 ratio/24-h interval, then it might be possible to capture additional peptide in the tumor. It is important to emphasize that just because there might be more bsMAb in the tumor, it does not guarantee that a larger fraction of the peptide will be captured. The very rapid clearance of the peptide limits the amount of peptide that will ever pass through the tumor to only a small fraction of the injected material. Thus, it is only necessary to have enough bsMAb in the tumor to optimize the probability of capturing a majority of this material. Having additional bsMAb in the tumor above this amount would not lead to further capturing of the radiolabeled peptide. In our model, it was estimated that if 50 times more bsMAb were given, it would take a 2-day interval before the moles of bsMAb in the blood would be at the same level as the 10:1/24-h interval. At this time, there would be 2.5× as much bsMAb in the tumor using the 50:1/48-h interval as compared with the 10:1/24-h interval.

To test this hypothesis, *in vivo* studies were performed using a fixed peptide dose of 0.05 nmol together with 10:1 and 50:1 bsMAb peptide ratios by injecting either 50 μg (0.5 nmol) of the bsMAb or 250 μg of the bsMAb (3 nmol), respectively. In addition to examining the 10:1/24-h and 50:1/48-h intervals, two other groups were included, 10:1/48-h and 50:1/24-h intervals, to assess the effects of longer or shorter intervals with a fixed peptide dose (0.05 nmol). Table 1 summarizes these findings. The bsMAb had similar distribution in the 10:1/24-h interval group as that seen in previous studies with 3.8 ± 0.73% ID/g in the tumor measured 3 h after the peptide injection. Peptide uptake in the tumor at this time averaged 18.4 ± 4.2% ID/g, and T/NT ratios for the peptide in the liver, lungs, and blood were greater than 15:1. Twenty-four h later, tumor uptake of the peptide was 14.2 ± 3.2% ID/g, with no appreciable change in the T/NT ratios, except that there was a significant

improvement in the tumor/blood ratio to 57.6 ± 10.8 compared with 15.7 ± 6.6 at 3 h ($P = 0.0007$). Three h after the radiolabeled peptide injection in the 50:1/48-h group, the %ID/g of the bsMAb in the tumor was reduced by 34% compared with the value 1 day earlier (2.49 ± 0.34% ID/g; $P = 0.031$), but because 5-fold more moles of bsMAb were injected, there were more moles of bsMAb in the tumor, which subsequently resulted in a 60% higher peptide uptake in the tumor, increasing to 29.2 ± 5.1% ID/g ($P = 0.016$). The higher tumor uptake in the 50:1/48-h interval group, combined with somewhat less uptake in the normal tissues, resulted in higher T/NT ratios.

The other groups of animals included in this study reinforced our earlier findings. For example, when the interval was extended to 48 h in the 10:1 bsMAb/peptide ratio group, tumor uptake of the peptide decreased by nearly 50% of that seen in the animals given the peptide after 24 h. Thus, with about 2-fold less bsMAb in the tumor, less peptide was targeted. However, as shown in the earlier example, the tumor/blood ratio in this group of animals was higher compared with the 10:1/24-h interval group. The 50:1/24-h interval group was interesting for several reasons. First, the %ID/g of the bsMAb and the peptide in the tumor were the same as that seen in the 10:1/24-h interval group, but there was also a higher amount of the peptide in all normal tissues. Therefore, T/NT ratios were less in the 50:1/24-h interval group. Secondly, unlike all of the other pretargeting groups that showed a loss in the amount of bsMAb and peptide in the tumor at 24 h, in this group, the %ID/g of the peptide and bsMAb in the tumor remained at a similar level as that seen at 3 h. The most likely explanation for this was that the peptide formed a complex with two bsMAb, thereby slowing the bsMAb clearance from the blood and giving it more time to localize in the tumor.

### *Tumor Size and Pretargeting*

During the course of examining these pretargeting issues, very often peptide uptake was higher in larger tumors (*e.g.,* >0.2 g) than in smaller tumors (*e.g.,* ≤0.1 g). This was interesting because, based on findings by our group (38, 42) and others (43, 44) with directly radiolabeled antibodies, a higher %ID/g is typically observed in smaller tumors rather than in larger tumors. A separate study was devised to specifically examine this issue by injecting the bsMAb in animals that had smaller (*e.g.,* ~0.1 g) compared with larger tumors (~0.3–0.5 g). All mice were given 15 μg of the bsMAb followed 24 h later by the $^{111}$In-IMP-241 using the 10:1 bsMAb/peptide ratio. The %ID/g for the bsMAb was similar in all tumors (*e.g.,* 3.1 ± 1.2 and 3.8 ± 0.4 in the small and large tumors, respectively) and tissues (*e.g.,* 0.8 ± 0.1 and 1.1 ± 0.3% ID/g in the animals with small and large tumors, respectively), regardless of the tumor size in the animals, but as shown in Fig. 7, the % ID/g of the peptide in the larger tumors (19.7 ± 2.1) was nearly 2-fold more than that of the peptide in the smaller tumors (8.53 ± 5.2). The large SD in the small tumor group reflected the finding that one of these tumors did have a %ID/g of the peptide similar to that of the larger tumor group (*i.e.,* 17.4% ID/g *versus* 4.6–8.2% ID/g in the other four animals). Thus, occasionally, substantial peptide uptake can occur in a small tumor, but more often there is a lower uptake than that seen in larger tumors. This study was repeated, this time giving nude mice bearing either 0.11 ± 0.04-g tumors or 0.47 ± 0.09-g tumors 400 μg of the bsMAb, followed 24 h later with the radiolabeled peptide, using a bsMAb/peptide mole injection ratio of 10:1. The same findings occurred; namely, the %ID/g was 2-fold higher in the larger tumors than in the smaller tumors (data not shown). The higher %ID/g of the radiolabeled peptide in the larger tumors could simply represent the fact that there were more moles of bsMAb in the larger tumors than in the smaller ones, as seen by the difference in the percentage of injected dose in the total tumor mass for the larger tumors (1.56 ± 0.31) compared with the smaller tumors (0.34 ± 0.16). Thus, with more moles of bsMAb available in the tumor, more peptide will be bound. Tumor physiology can also contribute to this finding. For example, at necropsy, the smaller GW-39 tumors were characterized as a very white, loosely connected mass, whereas the 0.4-g tumors were pink in color, suggesting better vascularization, and more tightly formed. Histological examination of these masses revealed these larger tumors to have well-defined vascular channels throughout, whereas tumors of <0.1 g had few internal vascular structures, with blood vessels predominantly at the perimeter. Because the peptide is cleared from the blood very quickly, tumors with a good blood supply would be more likely to have a portion of the peptide circulate through them, whereas those with a more limited blood supply would be expected to have a smaller fraction of the total injected peptide pass through them. In contrast, a large, slowly clearing macromolecule, such as a whole IgG, stays in the circulation a longer time, giving additional opportunities for tumors with more limited blood supply to be exposed to antibody.

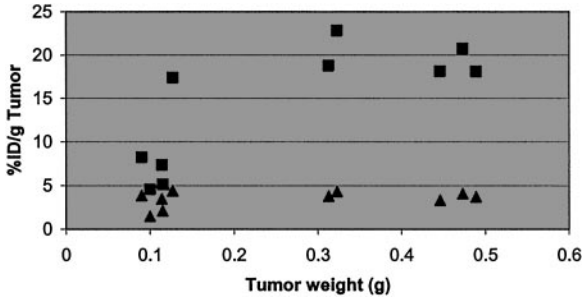


*Fig. 7* Peptide pretargeting: dependency on tumor size. Two groups of nude mice bearing different-sized GW-39 xenografts received injection with 15 μg of hMN-14 × m679 F(ab′)$_2$ bsMAb. Twenty-four h later, mice received injection with $^{111}$In-IMP-241 (10:1 bsMAb/peptide mole injection ratio). The animals were all necropsied 3 h after the peptide injection, and the %ID/g in tumor was determined (■, $^{111}$In-peptide; ▲, $^{125}$I-bsMAb).

### *Multiple Injections/Fractionation*

Other strategies that might improve pretargeting include giving multiple injections of either the peptide or both the bsMAb and the peptide. Because the peptide is cleared so quickly from the blood, it might be possible to load additional peptide into a tumor by giving multiple injections of the peptide after a single bsMAb injection. As long as the peptide injection is given when there is minimal amount of bsMAb in the blood, as in our standard model, nearly 90% of the peptide is cleared from the body in just 2 h. Thus, additional injections of the

*Table 2* Fractionation of the radiolabeled peptide after a single injection of the bsMAb

A. Single injection of 1.0 mCi of peptide

| Hours | %ID/g | μCi injected | μCi in tumor (effective) |
|---|---|---|---|
| 3 | 14.7 | 1000 | 142 |
| 6 | 13.3 | 1000 | 125 |
| 24 | 8.9 | 1000 | 68 |
| 48 | 6.0 | 1000 | 36 |
| | | Total | 371 |

B. 2 × 500 μCi injections of the peptide spaced 3 h apart

| | Contribution from Injection 1 | | | Contribution from Injection 2 | | | |
|---|---|---|---|---|---|---|---|
| Hours | %ID/g | μCi injected | μCi in tumor (effective) | %ID/g | μCi injected | μCi in tumor (effective) | Injection 1 + 2 (μCi) |
| 3 | 14.7 | 500 | 72.2 | 0 | 500 | 0 | 72.2 |
| 6 | 13.3 | 500 | 62.3 | 6.6 | 500 | 32.0 | 94.3 |
| 24 | 8.9 | 500 | 34.2 | 4.9 | 500 | 24.5 | 53.6 |
| 48 | 6.0 | 500 | 17.8 | 4.3 | 500 | 21.7 | 31.1 |
| | | | | | | Total | 251.2 |

peptide could be given sequentially over a few hours. Because, in our model, the amount of bsMAb in the tumor decreases by about 30–50%/day, delaying peptide injections over several days did not seem to be practical, and thus more closely spaced injections were examined. Because the doses of radioactivity were closely spaced, we assumed that the total amount of radioactivity injected could not exceed the amount given as a single bolus dose without having substantially more toxicity. Thus, the study was designed to compare the delivery of the same amount of radioactivity given as a single peptide injection or as two equal fractions. For a single injection of the peptide, animals were given 366 μg of the bsMAb (3.66 nmol), and 24 h later, 0.366 nmol of peptide containing a tracer amount of $^{111}$In-IMP-241 (40 μCi) was injected. Animals were necropsied at 3, 6, 24, and 48 h after the peptide injection. In the fractionated regimen, the same amount of bsMAb was injected, but the peptide injection was split into two fractions, each containing 0.366 nmol, given 3 h apart. This group was evaluated in two different ways, by either including a radiotracer amount of $^{111}$In-IMP-241 (40 μCi) in each peptide injection or giving a prescribed amount of unlabeled peptide in the first dose and then including the radiotracer in the second injection. Similar results were seen for each of these studies, but the latter method better illustrates the underlying process. In this second method, animals were necropsied at 3, 21, and 45 h after the last peptide injection, and we used the data from the single injection group to estimate the amount of peptide delivered after the first injection over the given time course. Table 2 shows the %ID/g (biological) of the radiolabeled peptide in the tumor for each of the necropsy time intervals, along with a calculation of the amount of radioactivity that would be in the tumor if a single 1.0-mCi dose of peptide were given or if the peptide had been fractionated in half, with two equal 0.5-mCi doses. Three h after a single injection of the peptide, there was 14.7% ID/g of the peptide in the tumor, which if 1.0 mCi were injected, would be 142 μCi in the tumor. The amount of the peptide in the tumor gradually decreases, and at the end of the 48-h monitoring period, a total of 371 μCi was accounted for in the tumor. For the fractionated scheme, where the radiotracer dose was only given with the second injection, we assumed that the %ID/g in the tumor would remain the same as for the first injection. Because only 50% of the radioactivity is administered, only half the amount of radioactivity is deposited in the tumor over this same time course. From this perspective, it is easy to see that in order for this fractionated scheme to deliver at least the same amount of peptide to the tumor, the uptake of the peptide of the second injection had to equal that of the first injection. However, the %ID/g delivered to the tumor by the second injection was only 6.6% ID/g. As a result, the total amount of radioactivity delivered to the tumor in this fractionated setting was only 251.2 μCi, a 30% decrease over that which could be delivered by a single injection. A similar decrease in total radioactivity in the tumor was seen when both peptide injections contained the radiotracer dose. We attribute the lower % ID/g delivered in the second injection to the possibility that the most accessible bsMAb was bound by the first injection, reducing the probability for binding by the second injection. Examination of the mole ratio of peptide to bsMAb in the tumor indicated that approximately 30–40% of the bsMAb was bound by the peptide after the first injection, assuming only monovalent binding of the peptide. Thus, if each mole of peptide was actually bound to 2 moles of bsMAb, nearly 60–80% of the bsMAb would have been occupied in the tumor at the time of the second peptide injection.

It is again important to emphasize that this fractionation scheme increases the moles of peptide delivered to the tumor because, in this example, twice the number of moles of peptide were actually administered compared with the single injection. Had we split the peptide injection into two equal amounts based on moles injected, the bsMAb/peptide ratio for the first injection would have been 20:1 instead of 10:1, and therefore we would have had to modify the interval spacing; otherwise, the targeting results would have resembled that seen earlier. Instead, the bsMAb/peptide ratio was actually given at a 5:1 ratio. Thus, this study verifies that additional peptide can be loaded into the tumor by giving sequential peptide injections after a single

injection of the bsMAb, but it is unlikely that there would be significant gains in the total amount of radioactivity that could be delivered by this type of injection strategy. Indeed, the total amount of radioactivity delivered to the kidneys in each fraction was identical. Therefore, with less radioactivity delivered to the tumor but the same amount of radioactivity delivered to the kidneys, the tumor/kidney radiation dose ratios would decrease if such an approach were used.

An alternate fractionation strategy involves giving more than one injection of the bsMAb followed each time with a peptide injection (*e.g.,* a bsMAb/peptide cycle). For this approach, we did not investigate the administration of multiple cycles of the bsMAb and peptide repeated over weeks or months, but rather over a short interval, so that the multiple injection cycles would resemble a single injection regimen with the primary objective being to increase the length of time that the radioactivity resides in the tumor. Replenishing the tumor with new bsMAb might also overcome the gradual loss of bsMAb from the tumor over time. However, the cycling of bsMAb/peptide injections must be timed to allow for sufficient clearance of each agent to optimize the approach. With the bsMAb rapidly clearing from the blood, this method is feasible. Because the peptide can be given just 24 h after the bsMAb, and because the peptide clears so quickly, we elected to examine conditions where a second bsMAb injection was given just 3 h after the first peptide injection, followed 24 h later with the peptide injection. In addition, we examined cycle spacing, where the second bsMAb was given 1 or 7 days after the first peptide injection, with the peptide given 24 h after each bsMAb injection. For modeling, a comparison was made between a single dose of radioactivity and the same dose split into two equal fractions. Necropsy times after each of these fractionated schemes are indicated in Fig. 8, and the effective AUCs are provided in Table 3.

The extended distribution study for a single cycle of the bsMAb/peptide (Fig. 8*A*) shows the rapid uptake of the radiolabeled peptide just 3 h after its injection. There is then a gradual decrease in the amount of peptide in the tumor over 7 days. The effective AUC for this group was 463 μCi-h/g. When a second cycle of bsMAb is started 7 days after the first cycle, there is not much residual radioactivity remaining in the tumor to contribute to the total activity. Thus, the uptake of the peptide after the second bsMAb/peptide cycle with a 7-day spacing between cycles should have appeared the same as that observed for the first cycle. However, the %ID/g of the radiolabeled peptide in the tumor after this second cycle (Fig. 8*C*) was lower than that seen in the first cycle, which may have been due to tumor growth that had nearly doubled by the time the second cycle was given. When the radioactivity is expressed as μCi in the total tumor mass, the percentage of the injected dose in the tumors was identical for the first and second cycles (data not shown). The calculated AUC for the 7-day spacing cycle was at best only slightly higher (496 μCi-h/g) than that seen for a single cycle. In contrast, when the second cycle was initiated 24 h after the completion of the first cycle (48-h spacing between the two peptide doses), there was still a substantial amount of the radioactivity from the first injection remaining in the tumor, and thus the radioactivity delivered by the second injection added to this total amount (Fig. 8*B*). Unlike when only the peptide was

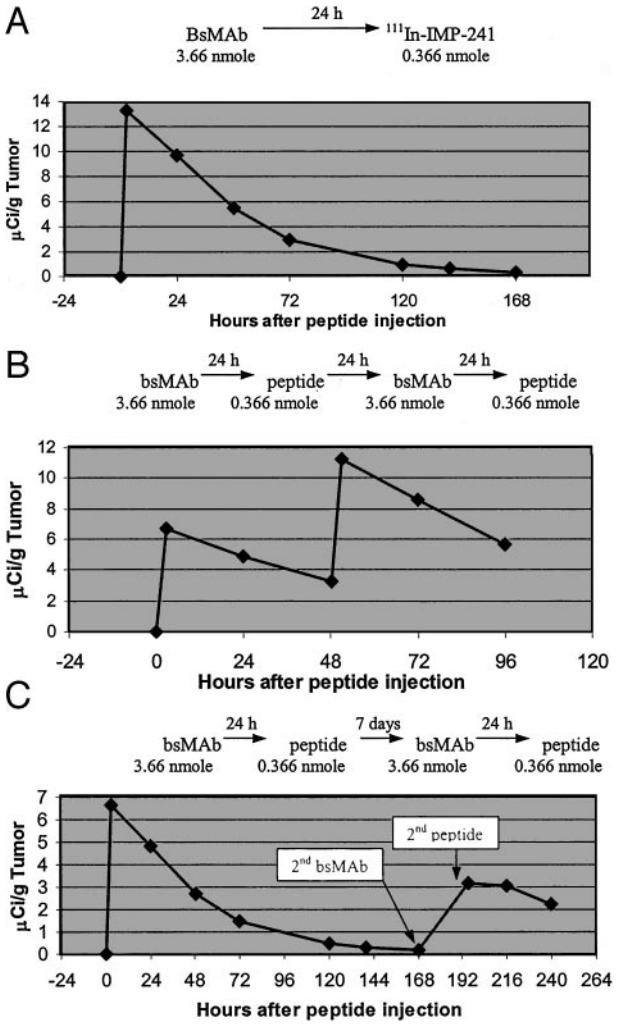


*Fig. 8* Fractionated cycles of bsMAb and peptide. Nude mice bearing GW-39 tumors were given a single injection of the bsMAb followed 24 h later with $^{111}$In-IMP-241 (*A*). In *B* and *C*, the animals were given $^{111}$In-IMP-241 for the first peptide injection and a second dose of $^{111}$In-IMP-241 for the second peptide injection, with each dose containing the prescribed moles of peptide as indicated. The timing of the second bsMAb was either 1 or 7 days after the first peptide injection (*B* and *C*, respectively). Groups of five animals were necropsied at the times indicated.

fractionated after a single injection of the bsMAb, where the %ID/g delivered by a second peptide injection was nearly 2-fold less than that seen after the first injection, the second injection of the bsMAb localized 1.7 ± 0.4% of the second bsMAb to the tumor, and subsequently 9.1 ± 1.7% ID/g of the peptide was localized at 3 h. This additional boost in radioactivity delivery to the tumor increased the AUC to 598 μCi-h/g for this fractionated injection without increasing the amount of radioactivity delivered to the normal tissues. Thus, this type of fractionation scheme might be beneficial. However, care must be taken in the timing of multiple cycles. Data for the group of animals that received the second injection of the bsMAb just 3 h after the first peptide injection indicated a slight increase in the amount

*Table 3* Evaluation of single *versus* fractionated cycles of bsMAb and peptide

Nude mice bearing GW-39 tumors (starting at 0.3–0.6 g) received i.v. injection with 366 μg (3.66 nmol) of the hMN-14 × m679 $F(ab')_2$ bsMAb. For the single cycle group, animals received a single injection of 0.366 nmol of $^{111}$In-IMP-241 (40 μCi) and were necropsied over 7 days. For the fractionated groups, mice first received 366 μg of the bsMAb followed 24 h later with 0.366 nmol of $^{111}$In-IMP-241. Then, at 3 h (3/27 h), 24 h (24/48 h), or 7 days (7/8 days) later, a second injection of 3.66 nmol of the bsMAb was given, followed 24 h later with 0.366 nmol of $^{111}$In-IMP-241 peptide. Animals were necropsied starting at 3 h after each peptide injection and then at the times indicated in Fig. 8. In the case with fractionated injections, the initial $^{111}$In-IMP-241 and $^{125}$I-bsMAb counting standards were supplemented at the time of the second injection with a dilution of the radiolabeled products, so that the total radioactivity (decayed from the first injection) + (newly injected radioactivity) given for both injections could be accounted for.

| | Effective AUC (μCi-h/g) | | | |
|---|---|---|---|---|
| | | Fractionation (bsMAb/peptide timing[a]) | | |
| | Single | 3/27 h | 24/48 h | 7/8 days |
| Tumor | 463 | 558 | 598 | 496 |
| Kidney | 36 | 88 | 46 | 39 |
| Liver | 133 | 154 | 128 | 150 |
| Blood | 22 | 26 | 22 | 22 |

[a] First time indication is the time between the first peptide injection to the second bsMAb injection. The second time indication is the time between each peptide injection.

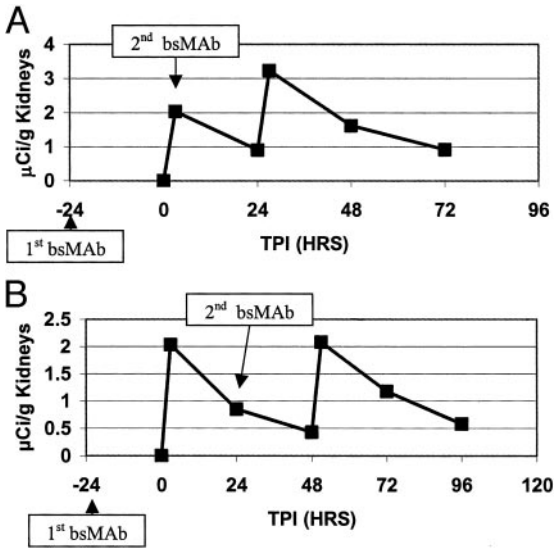


*Fig. 9* Radioactivity uptake in the kidney using fractionated cycles of bsMAb and peptide given over a 24- or 48-h interval spacing. In *A*, 24 h after the first bsMAb was given, the first peptide injection was given, and radioactivity determinations were made 3 and 24 h after this injection. A separate group of animals was given a second bsMAb injection 3 h after the first peptide injection and then received a second peptide injection 24 h later. This represents a 24-h interval between the two peptide doses. In *B*, a separate group of animals had the second bsMAb delayed until 24 h after the first peptide injection. This represents a 48-h interval between the two peptide doses. Tumor uptake for this group of animals is shown in Fig. 8*B*.

of peptide in most of the normal tissues, as reflected in the higher AUCs calculated for the normal tissues (Table 3). This suggests that if the second bsMAb is given too soon, this bsMAb can potentially bind to the bsMAb/peptide complexes formed after the first injection. As discussed earlier, this would change the molecular size of these complexes, slowing their clearance rate from the blood and potentially increasing their deposition in the liver or spleen. Thus, sufficient time must be given between cycles to allow for the clearance of not only the peptide but also the bsMAb/peptide complexes. Proper spacing is also important for reducing radiation exposure to the kidneys. As shown in Fig. 9, when the second bsMAb cycle was started just 3 h after the first peptide injection, there was still sufficient residual radioactivity in the kidneys left from the first peptide injection at the time of the second peptide injection to increase the total dose delivered to the kidneys. However, delaying the second bsMAb cycle for 1 day after the first peptide injection allowed for sufficient reduction in the residual activity in the blood so that there was no real effective addition to the radiation-absorbed dose to the kidneys.

## Discussion

Pretargeting approaches are attractive alternatives to using directly radiolabeled antibodies, primarily because T/NT ratios that develop in just a few hours after the radiolabeled effector molecule far exceed those that can be obtained with a directly radiolabeled IgG and, in many instances, even antibody fragments. Indeed, as shown here and elsewhere (29), unless antibody fragments or other engineered constructs, such as scFv, are radioiodinated, there is a substantial localization of the radioactivity in the kidneys. However, with pretargeting and a properly designed peptide, renal retention is minimized. Thus, a pretargeting approach might be ideally suited for imaging applications, with the only caveat being that the entire procedure is a multiday process. Although rapid assessment of tumor targeting is important, there are a number of situations where a delay of a few days would not seriously interfere with the management of the disease, and therefore an appropriate antibody-directed pretargeting method that might enhance targeting sensitivity and specificity would be attractive.

Therapeutic applications for pretargeting have also been examined. Here again, the superior T/NT ratios achieved with pretargeting methods are very important. Because these ratios can be achieved within just a few hours after the radiolabeled agent is injected, compared with 1–2 days to reach maximum accretion for a radiolabeled antibody (45, 46), a larger fraction of the radiation dose can be deposited in the tumor than in normal tissues before it decays. Fig. 10 illustrates the biological and effective data derived for $^{111}$In-DOTA-hMN-14 IgG (effective data based on $^{90}$Y), compared with data modeled from the extended biodistribution data shown in Fig. 8*A* for a single injection of a $^{90}$Y-labeled peptide after the hMN-14 × m679 $F(ab')_2$ bsMAb. The biological data for the directly radiolabeled IgG show that it has a higher %ID/g and a longer retention in the tumor compared with the pretargeted $^{90}$Y-peptide. However, the percentage uptake in the blood and kidneys was lower for the pretargeting approach. To obtain a better appreciation of the therapeutic potential for each of these approaches, it is better to plot data based on the amount of radioactivity in the tissues

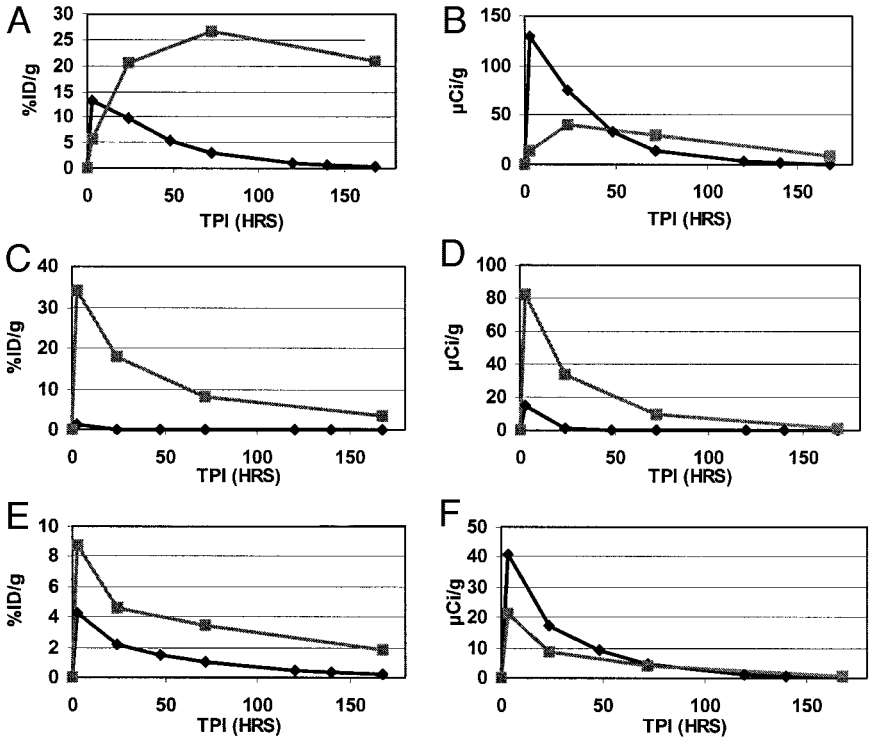


*Fig. 10* Biological and effective clearance curves comparing the uptake of an $^{111}$In ($^{90}$Y)-labeled IgG to an $^{111}$In ($^{90}$Y)-labeled peptide delivered by pretargeting. Data for the pretargeting study were taken from Fig. 8*A*. $^{111}$In-DOTA-hMN-14 IgG (10 μCi, 50 μg) was injected i.v. in GW-39 tumor-bearing nude mice (tumor size averaged 0.7–1.2 g at the time of necropsy). Animals were necropsied at 3, 24, 72, and 168 h later ($n$ = 4–5 animals/interval). *Panels* on the *left* are the %ID/g (biological), whereas *panels* on the *right* reflect the amount of radioactivity per gram tissue (*i.e.*, effective), assuming the injection of 0.25 mCi of $^{90}$Y-hMN-14 IgG (▨) or 1.0 mCi of $^{90}$Y-peptide (♦). *A* and *B,* tumor; *C* and *D,* blood; *E* and *F,* kidneys.

under therapeutic conditions. If the MTD was assumed to be 1.0 mCi for the pretargeted $^{90}$Y-peptide and 0.25 mCi for $^{90}$Y-IgG, the pretargeted $^{90}$Y-peptide would deposit more radioactivity in the tumor at earlier times (Fig. 10*B*). Although this would result in a higher dose rate than the $^{90}$Y-IgG (*e.g.,* 57.8 *versus* 31.4 μCi/g·h$^{-1}$ over 72 h for pretargeting *versus* IgG, respectively), the AUCs for these effective curves were similar (4635 *versus* 4780 for the $^{90}$Y-peptide and $^{90}$Y-IgG, respectively), and thus the total radiation dose would be similar. Other studies comparing radiolabeled whole IgG with antibody fragments have suggested that improvements in tumor responses may be explained by a higher dose rate (47, 48), but a more uniform distribution in the tumor by smaller fragments could also explain some of this effect. Importantly, the extended biodistribution data used for these effective curves were generated based on the pretargeting data of a 10:1 bsMAb/peptide ratio with a 24-h spacing. Because we have shown a capability of nearly doubling the tumor uptake of the radiolabeled peptide without affecting normal tissue uptake by increasing the bsMAb dose (*i.e.*, 50:1/48-h spacing), this should give the pretargeting method an advantage not only for the radiation dose rate but also the total accumulated dose. The effective curves also illustrate that higher radiation doses would be delivered to the kidneys at the MTD of a $^{90}$Y-peptide than with the MTD of $^{90}$Y-IgG, whereas the radiation dose to the red marrow (as illustrated by blood concentrations) would be remarkably lower. Thus, care will need to be taken to ensure careful monitoring of renal function.

It is important both for imaging and therapy to optimize the amount of the injected radioactivity in the tumor. For imaging, this will enhance the count rate in the tumor, which improves image resolution; for therapy, a larger fraction of the radioactivity delivered to the tumor will increase the radiation-absorbed dose. This can be quite a challenge for a molecule that naturally clears quickly from the blood. With a limited number of passages through a target lesion and a decreasing concentration over a short time, rapidly clearing molecules (*e.g.,* peptides) will typically accumulate at a lower concentration in a target lesion than a molecule that remains in the circulation for a longer period of time (*e.g.,* whole IgG). Increasing the total injected dose of a rapidly clearing molecule will allow a greater mass to pass through the target lesion, which can in some degree compensate for its rapid clearance. However, this total injected dose would be limited by the toxicity to the organ involved in clearing this agent from the body or possibly another organ that would be more susceptible to the toxicity. Thus, processes that optimize the amount of the agent targeted to lesions without compromising normal tissue accretion are critical to the success of a therapeutic application. In this regard, we have carefully reviewed the targeting properties of a bsMAb pretargeting system that will use a radiolabeled peptide prepared with radionuclides that are stably bound by DOTA (*e.g.,* $^{90}$Y, $^{177}$Lu) for therapy. Although a number of studies were performed, we have restricted the results presented herein to those that could help improve a process that might be used to optimize other pretargeting systems.

The first issue that must be addressed is the clearance and targeting properties of the bsMAb by itself. Critical to this assessment is the need to examine a range of bsMAb protein doses that might be used for therapy. Included in these studies should be an examination of whether a particular protein dose range would saturate antigen sites in the tumor. If all antigen sites in the tumor are bound by the bsMAb, theoretically this

condition should allow for maximum peptide binding. However, this is not to say that maximum peptide uptake will occur only if the maximum amount of bsMAb is loaded in the tumor. In a pretargeting procedure, the peptide clears very rapidly from the blood, which means that only a small fraction of the peptide will pass through the tumor. Because the moles of peptide injected for imaging or radionuclide therapy would be fixed (*e.g.,* based on the radionuclide MTD), it is likely that there is an optimum threshold of bsMAb necessary to optimize the capturing of this amount of peptide. Injecting more bsMAb would not be harmful to the overall pretargeting process, but it would require additional time to allow for the bsMAb to clear from the blood and tissues before the peptide is injected. Finally, having a sufficient excess of bsMAb in the tumor should also increase the peptide's retention time in the tumor, because this would provide greater assurance that the bsMAbs were positioned in close enough proximity to allow the bridging of the divalent hapten.

During the course of this investigation, we found unexpectedly that when tumors were smaller in size, the targeting of radiolabeled peptide was frequently less than that for tumors of somewhat larger size. Because several targeting studies over many years with directly radiolabeled antibodies have reported a higher %ID/g for smaller rather than larger tumors (38, 43), we investigated this further. The results of a controlled study where animals were grouped by tumor size (tumor $\leq$ 0.1 g *versus* tumor $\geq$ 0.2 g) confirmed this finding; namely, smaller tumors were more likely to have a lower %ID/g than larger ones. As discussed earlier, this could be the result of the combination of a limited tumor blood supply in the smaller tumors and the rapidly clearing peptide. It is uncertain whether this finding would have any significance to therapeutic responses of smaller tumors; because there is still a substantial fraction of the radioactivity delivered to the smaller tumors, we suspect the impact is minimal. Nevertheless, it is important to at least be cognizant that this situation might occur when examining other pretargeting approaches in other model systems.

For optimizing pretargeting, the most important issues to examine are the interval spacing between the bsMAb and the peptide and the ratio of these two agents. As these studies show, there is considerable integration between these two parameters. We found it convenient to first proceed from an understanding of how much peptide will be used for a given application. Once the peptide dose is fixed, the interrelationship between the bsMAb protein dose and interval spacing needs to be assessed. We tested several model systems in addition to the one reported here, and in each instance, a good starting point proved to be a bsMAb/peptide mole injection ratio of 10:1 and to delay the injection of the peptide until there was $<$1.0% ID/g of the bsMAb in the blood. We elect to use the mole ratio of bsMAb and peptide that was injected simply because it was convenient, and in this model system, the clearance rate of the bsMAb is fairly predictable. In situations where bsMAb clearance is highly variable, then it would be more appropriate to measure the bsMAb concentration before peptide injection. By starting with an examination of how targeting is influenced by adjusting the interval spacing using a 10:1 ratio, sufficient insight should be gained to gauge how a given system performs and what the optimal interval spacing for this ratio would be. Our experience has shown that it is not always possible to administer the peptide at the time when the highest amount of bsMAb is in the tumor; instead, it is more important to adjust the timing to reduce the amount of peptide bound by bsMAb remaining in the blood.

Once an understanding of the interrelationships at a given bsMAb/peptide injection ratio and interval is known, it is important to re-evaluate whether increasing the bsMAb dose and interval spacing will improve peptide targeting. By knowing how many moles of bsMAb are in the blood at a given interval and the peptide dose that produces reasonable targeting data, the prospects that increasing bsMAb will lead to improved tumor uptake can be calculated in advance and then tested. Data expressed as the %ID/g do not lend themselves to the best understanding of the pretargeting process, and therefore these data should be converted to moles or even molar concentrations. The more substantial the difference between the amount of bsMAb in the tumor and the blood, the better the chances that peptide uptake in the tumor will improve with increasing bsMAb doses. This is the principal behind the optimization of the streptavidin-biotin pretargeting system reported by Axworthy *et al.* (14, 15), which provided insights on how a pretargeting system could be optimized for a therapeutic setting. In this system, an agent is used to remove and, at the same time, block the biotin-binding sites of the streptavidin-antibody conjugate before the administration of the radiolabeled biotin. Even if this clearing step results in the partial loss of the conjugate in the tumor, if the differential loss in the blood is greater than that in the tumor, pretargeting will be more successful. In this situation, by administering higher doses of the conjugate, the loss of conjugate from the tumor that occurs during the period of time between the clearing agent and the time of the radiolabeled biotin can be compensated for. The agent used to clear and simultaneously block biotin binding sites was necessary in this system because the large molecular size of the IgG-streptavidin conjugate clears slowly from the blood. If the radiolabeled biotin injection were delayed until the level of the conjugate in the blood was low, tumor uptake would have likely decreased significantly. Indeed, without a clearing step, the delay could be measured in weeks, which could increase the uncertainty of the quality of the conjugate localized in the tumor, especially because there is endogenous biotin in blood and tissues that would eventually bind to the sites on the tumor-localized streptavidin, thereby preventing the binding of the radiolabeled biotin. We found an analogous situation when an IgG $\times$ Fab′ bsMAb was compared with a F(ab′)$_2$ $\times$ Fab′ and Fab′ $\times$ Fab′ bsMAb as pretargeting agents. The IgG $\times$ Fab′ bsMAb had a concentration in the tumor nearly 5–10 times that which could be achieved with Fab′ $\times$ Fab′ or even F(ab′)$_2$ $\times$ Fab′ bsMAb conjugates, yet because of its protractedly high concentration in the blood, the peptide injection had to be delayed until a time when its concentration in the tumor was only equal to that of the F(ab′)$_2$ $\times$ Fab′ bsMAb at the optimal time for administering the peptide for this conjugate (41). We also evaluated a variety of agents that could either clear, block, or clear and block a bsMAb from the blood in an attempt to use an IgG $\times$ Fab′ bsMAb conjugate (41). Despite using a number of different strategies to either clear, block, or block and clear the bsMAb remaining in the blood, the best that could be achieved was parity with the results obtained with the F(ab′)$_2$ $\times$ Fab′ conjugate that naturally cleared more quickly. This experience certainly does not dis-

count the possibility that a clearing/blocking agent could be developed for a bsMAb approach, but it highlights the difficulties encountered in this process. Thus, it would greatly simplify pretargeting if a clearing step were not necessary.

We believe the best solution lies in the development of recombinant bsMAb. These molecules can be prepared with a smaller molecular size than these chemical conjugates, but with similar binding affinities/avidities. Their configuration can be adjusted to have more than one binding site for the tumor antigen or even the hapten. In part as an exercise in proof of principal, our group prepared a bispecific diabody against CEA and HSG (49). This diabody, BS1.5, was shown to have similar binding affinity for CEA and HSG as the chemically constructed Fab′ × Fab′ bsMAb starting from hMN-14 anti-CEA and the murine 679 anti-HSG IgG. However, at a molecular weight of only ~50,000, compared with about $M_r$ 100,000, the bispecific diabody cleared much more rapidly from tumor-bearing animals, but tumor uptake was the same at an earlier time. Thus, when used as a pretargeting agent, tumor uptake of the radiolabeled peptide was the same for the bispecific diabody and the Fab′ × Fab′, but because there was less BS1.5 in the blood and normal tissues, superior T/NT ratios were achieved. We also prepared the fully humanized version of this bispecific diabody (BS1.5H) and have demonstrated binding properties similar to those of the chemically conjugated bsMAb (49). This investigation clearly shows that recombinant bispecific antibodies can be made with similar binding properties but also with more favorable pharmacokinetics that improve their utility as pretargeting agents. These agents would also be more easily and economically manufactured than having to prepare chemical conjugates from two different cell lines. All of these factors alone make recombinant bispecific antibodies more attractive than chemical conjugates for clinical development. However, the innovation and improvements do not stop with the bispecific diabody because, as we have shown, it is also possible to make bispecific antibodies that have two binding sites for CEA and one against HSG, but again with a smaller molecular size than could be prepared by chemical conjugation (49). Although it is conceivable to make more exotic constructs, there are still issues regarding purification of these types of constructs, as well as up-scaling their production, but it is only a matter of time before these issues are resolved, and these new targeting constructs will advance in development.

We also examined two different fractionation strategies for bsMAb pretargeting. Administering several injections of the radiolabeled peptide after a single injection of the peptide was not a useful approach because the concentration of the bsMAb in the tumor continues to decrease over time, and in each peptide injection, the fraction that is bound to the tumor decreased, but the fraction clearing through the kidney remained the same. The better approach was to repeat the cycle of bsMAb and peptide injections. By replenishing the amount of bsMAb in the tumor, the fraction of peptide captured each time can actually increase, but this is only achieved by careful timing between the cycles. In an optimal setting, a stepped increase in the amount of radioactivity delivered to the tumor can occur. Although this stepped increase did not occur when the spacing between the bsMAb/peptide cycles was 1 week, dosimetry-based predictions cannot account for possibilities of synergistic effects associated with a fractionated exposure to radiation.

Finally, a question that frequently arises is how predictable animal testing is for clinical translation. In the case of pretargeting approaches that require the optimization of several parameters, preclinical testing is essential because it can help direct the manner in which clinical trials should proceed. Animal testing shows the importance of properly adjusting the interval between the bsMAb and peptide to optimize pretargeting, which is responsible for establishing an appropriate bsMAb/peptide molar relationship. In mice, when the injected dose of the peptide was increased 10–20-fold and the bsMAb injected dose was increased to keep pace with the desired mole ratio, the %ID/g of the peptide in the tumor and normal tissue remained fairly constant. However, during this escalation process, there is evidence of a slow rise in the %ID/g peptide in the normal tissues, which would be expected, because by increasing the molar concentration of the bsMAb and peptide in the blood, conditions would become more favorable for them to interact at the point of their first contact (*i.e.*, the blood). In mice, peptide pretargeting was optimized when the moles of bsMAb per milliliter of blood was at least 8 times less than the moles of peptide to be injected, but at a 2:1 ratio, the peptide is more likely to bind to the bsMAb in the blood. A similar relationship should be found in humans, but because the volume of distribution in humans is higher, it will need to be determined empirically. Thus, these preclinical studies have a direct bearing on the initial steps needed to optimize this procedure clinically.

In conclusion, there are a number of issues to consider when developing a pretargeting procedure. Pretargeting methods are not as simple as administering a directly radiolabeled antibody, but as the studies herein show, a bsMAb pretargeting procedure that does not require a clearing agent can deliver as much and even more radioactivity to the tumor as the directly radiolabeled antibody and with less delivery of radioactivity to normal tissues. Therefore, we envision that bsMAb pretargeting procedures using recombinant bsMAb and peptides conjugated with a variety of radionuclides will gain an important role in the further development of methods of selectively imaging and treating cancer in the future.

## Acknowledgments

We thank Dr. Michele Losman, Guy Newsome, and Gaik Lin Ong for assistance in the preparation of the bsMAbs and Phil Andrews and Nick Kumburis for radiolabeling and quality assurance support.

## References

1. Pressman, D., and Korngold, L. The *in vivo* localization of anti-Wagner osteogenic sarcoma antibodies. Cancer (Phila.), *6:* 619–623, 1953.

2. Primus, F. J., Wang, F. H., Goldenberg, D. M., and Hansen, H. J. Localization of human GW-39 tumors in hamsters by radiolabeled heterospecific antibody to carcinoembryonic antigen. Cancer Res., *33:* 2977–2982, 1973.

3. Goldenberg, D. M., Preston, D. F., Primus, F. J., and Hansen, H. J. Photoscan localization of GW-39 tumors in hamsters using radiolabeled anti-carcinoembryonic antigen immunoglobulin G. Cancer Res., *34:* 1–9, 1974.

4. Mach, J. P., Carrel, S., Merenda, C., Sordat, B., and Cerottini, J. C. *In vivo* localisation of radiolabelled antibodies to carcinoembryonic

antigen in human colon carcinoma grafted into nude mice. Nature (Lond.), *248:* 704–706, 1974.

5. Goldenberg, D. M., DeLand, F., Kim, E., Bennett, S., Primus, F. J., van Nagell, J. R., Jr., Estes, N., DeSimone, P., and Rayburn, P. Use of radiolabeled antibodies to carcinoembryonic antigen for the detection and localization of diverse cancers by external photoscanning. N. Engl. J. Med., *298:* 1384–1388, 1978.

6. Goldenberg, D. M. An introduction to the radioimmunodetection of cancer. Cancer Res., *40:* 2957–2959, 1980.

7. Goldenberg, D. M., Gaffar, S. A., Bennett, S. J., and Beach, J. L. Experimental radioimmunotherapy of a xenografted human colonic tumor (GW-39) producing carcinoembryonic antigen. Cancer Res., *41:* 4354–4360, 1981.

8. Wagner, H. N., Jr., Wiseman, G. A., Marcus, C. S., Nabi, H. A., Nagle, C. E., Fink-Bennett, D. M., Lamonica, D. M., and Conti, P. S. Administration guidelines for radioimmunotherapy of non-Hodgkin's lymphoma with $^{90}$Y-labeled anti-CD20 monoclonal antibody. J. Nucl. Med., *43:* 267–272, 2002.

9. Chang, C. H., Sharkey, R. M., Rossi, E. A., Karacay, H., McBride, W., Hansen, H. J., Chatal, J. F., Barbet, J., and Goldenberg, D. M. Molecular advances in pretargeting radioimmunotherapy with bispecific antibodies. Mol. Cancer Ther., *1:* 553–563, 2002.

10. Reardan, D. T., Meares, C. F., Goodwin, D. A., McTigue, M., David, G. S., Stone, M. R., Leung, J. P., Bartholomew, R. M., and Frincke, J. M. Antibodies to metal chelates. Nature (Lond.), *316:* 265–268, 1985.

11. Hnatowich, D. J., Virzi, F., and Rusckowski, M. Investigations of avidin and biotin for imaging applications. J. Nucl. Med., *28:* 1294–1302, 1987.

12. Paganelli, G., Riva, P., Deleide, G., Clivio, A., Chiolerio, F., Scassellati, G. A., Malcovati, M., and Siccardi, A. G. *In vivo* labeling of biotinylated monoclonal antibodies by radioactive avidin: a strategy to increase tumor radiolocalization. Int. J. Cancer Suppl., *2:* 121–125, 1988.

13. Grana, C., Chinol, M., Robertson, C., Mazzetta, C., Bartolomei, M., De Cicco, C., Fiorenza, M., Gatti, M., Caliceti, P., and Paganelli, G. Pretargeted adjuvant radioimmunotherapy with yttrium-90-biotin in malignant glioma patients: a pilot study. Br. J. Cancer, *86:* 207–212, 2002.

14. Axworthy, D. B., Fritzberg, A. R., Hylarides, M. D., Mallet, R. W., Theodore, L. J., Gustavson, L. M., Su, F-M., Beaumier, P. L., and Reno, J. M. Preclinical evaluation of an anti-tumor monoclonal antibody/streptavidin conjugate for pretargeted $^{90}$Y radioimmunotherapy in a mouse xenograft model. J. Immunother., *16:* 158, 1994.

15. Axworthy, D. B., Reno, J. M., Hylarides, M. D., Mallett, R. W., Theodore, L. J., Gustavson, L. M., Su, F., Hobson, L. J., Beaumier, P. L., and Fritzberg, A. R. Cure of human carcinoma xenografts by a single dose of pretargeted yttrium-90 with negligible toxicity. Proc. Natl. Acad. Sci. USA, *97:* 1802–1807, 2000.

16. Press, O. W., Corcoran, M., Subbiah, K., Hamlin, D. K., Wilbur, D. S., Johnson, T., Theodore, L., Yau, E., Mallett, R., Meyer, D. L., and Axworthy, D. A comparative evaluation of conventional and pretargeted radioimmunotherapy of CD20-expressing lymphoma xenografts. Blood, *98:* 2535–2543, 2001.

17. Breitz, H. B., Fisher, D. R., Goris, M. L., Knox, S., Ratliff, B., Murtha, A. D., and Weiden, P. L. Radiation absorbed dose estimation for $^{90}$Y-DOTA-biotin with pertargeted NR-LU-10/streptavidin. Cancer Biother. Radiopharm., *14:* 381–395, 1999.

18. Breitz, H. B., Weiden, P. L., Beaumier, P. L., Axworthy, D. B., Seiler, C., Su, F. M., Graves, S., Bryan, K., and Reno, J. M. Clinical optimization of pretargeted radioimmunotherapy with antibody-streptavidin conjugate and $^{90}$Y-DOTA-biotin. J. Nucl. Med., *41:* 131–140, 2000.

19. Knox, S. J., Goris, M. L., Tempero, M., Weiden, P. L., Gentner, L., Breitz, H., Adams, G. P., Axworthy, D., Gaffigan, S., Bryan, K., Fisher, D. R., Colcher, D., Horak, I. D., and Weiner, L. M. Phase II trial of yttrium-90-DOTA-biotin pretargeted by NR-LU-10 antibody/streptavidin in patients with metastatic colon cancer. Clin. Cancer Res., *6:* 406–414, 2000.

20. Weiden, P. L., and Breitz, H. B. Pretargeted radioimmunotherapy (PRIT) for treatment of non-Hodgkin's lymphoma (NHL). Crit. Rev. Oncol. Hematol., *40:* 37–51, 2001.

21. Le Doussal, J-M., Martin, M., Gautherot, E., Delaage, M., and Barbet, J. *In vitro* and *in vivo* targeting of radiolabeled monovalent and divalent haptens with dual specificity monoclonal antibody conjugates: enhanced divalent hapten affinity for cell bound antibody conjugates. J. Nucl. Med., *30:* 1358–1366, 1989.

22. Le Doussal, J-M., Chetanneau, A., Gruaz-Guyon, A., Martin, M., Gautherot, E., Lehur, P-A., Chatal, J-F., Delaage, M., and Barbet, J. Bispecific monoclonal antibody-mediated targeting of an indium-111-labeled DTPA dimer to primary colorectal tumors: pharmacokinetics, biodistribution, scintigraphy and immune response. J. Nucl. Med., *34:* 1662–1671, 1993.

23. Gautherot, E., Le Doussal, J-M., Bouhou, J., Manetti, C., Martin, M., Rouvier, E., and Barbet, J. Delivery of therapeutic doses of radioiodine using bispecific antibody-targeted bivalent haptens. J. Nucl. Med., *39:* 1937–1943, 1998.

24. Gautherot, E., Rouvier, E., Daniel, L., Loucif, E., Bouhou, J., Manetti, C., Martin, M., Le Doussal, J-M., and Barbet, J. Pretargeted radioimmunotherapy of human colorectal xenografts with bispecific antibody and $^{131}$I-labeled bivalent hapten. J. Nucl. Med., *41:* 480–487, 2000.

25. Kraeber-Bodéré, F., Faivre-Chauvet, A., Saï-Maurel, C., Gautherot, E., Fiche, M., Campion, L., Le Boterff, J., Barbet, J., Chatal, J-F., and Thédrez, P. Bispecific antibody and bivalent hapten radioimmunotherapy in CEA-producing medullary thyroid cancer xenograft. J. Nucl. Med., *40:* 198–204, 1999.

26. Karacay, H. Sharkey, R. M., Griffiths, G. L., Govindan, S. V., McBride, W. J., Goldenberg, D. M., and Hansen, H. J. Development of a streptavidin-anti-carcinoembryonic antigen antibody, radiolabeled biotin pretargeting method for radioimmunotherapy of colorectal cancer: reagent development. Bioconjugate Chem., *8:* 585–594, 1997.

27. Sharkey, R. M., Karacay, H., Griffiths, G. L., Behr, T. M., Blumenthal, R. D., Mattes, M. J., Hansen, H. J., and Goldenberg, D. M. Development of a streptavidin-anti-carcinoembryonic antigen antibody, radiolabeled biotin pretargeting method for radioimmunotherapy of colorectal cancer. Studies in a human colon cancer xenograft model. Bioconjugate Chem., *8:* 595–604, 1997.

28. Karacay, H., McBride, W. J., Griffiths, G. L., Sharkey, R. M., Barbet, J., Hansen, H. J., and Goldenberg, D. M. Experimental pretargeting studies of cancer with a humanized anti-CEA × murine anti-[In-DTPA] bispecific antibody construct and a $^{99m}$Tc-/$^{188}$Re-labeled peptide. Bioconjugate Chem., *11:* 842–854, 2000.

29. Sharkey, R. M., McBride, W. J., Karacay, H., Chang, K., Griffiths, G. L., Hansen, H. J., and Goldenberg, D. M. A universal pre-targeting system for cancer detection and therapy using bispecific antibody. Cancer Res., *63:* 354–363, 2003.

30. Press, O. W., Eary, J. F., Appelbaum, F. R., Martin, P. J., Nelp, W. B., Glenn, S. Fisher, D. R., Porter, B., Matthews, D. C., Gooley, T., and Bernstein, I. D. Phase II trial of 131I-B1 (anti-CD20) antibody therapy with autologous stem cell transplantation for relapsed B cell lymphomas. Lancet, *346:* 336–340, 1995.

31. Kaminski, M. S., Zelenetz, A. D., Press, O. W., Saleh, M., Leonard, J., Fehrenbacher, L., Lister, T. A., Stagg, R. J., Tidmarsh, G. F., Kroll, S., Wahl, R. L., Knox, S. J., and Vose, J. M. Pivotal study of iodine I 131 tositumomab for chemotherapy-refractory low-grade or transformed low-grade B-cell non-Hodgkin's lymphomas. J. Clin. Oncol., *19:* 3918–3928, 2001.

32. Kraeber-Bodéré, F., Faivre-Chauvet, A., Ferrer, L., Vuillez, J-P., Brard, P-Y., Rousseau, C., Resche, I., Devillers, A., Laffont, S., Bardiès, M., Chang, K., Sharkey, R. M., Goldenberg, D. M., Chatal, J-F., and Barbet, J. Pharmacokinetics and dosimetry studies for optimization of anti-carcinoembryonic antigen × anti-hapten bispecific antibody-mediated pretargeting of iodine-131-labeled hapten in a Phase I radioimmunotherapy trial. Clin. Cancer Res., *9* (Suppl.)*:* 3973s–3981s, 2003.

33. Sharkey, R. M., Juweid, M., Shevitz, J., Behr, T., Dunn, R., Swayne, L. C., Wong, G. Y., Blumenthal, R. D., Griffiths, G. L., Siegel, J. A., Leung, S., Hansen, H. J., and Goldenberg, D. M. Evaluation of a

complementarity-determining region-grafted (humanized) anti-carcinoembryonic antigen monoclonal antibody in preclinical and clinical studies. Cancer Res., *55* (Suppl.)*:* 5935s–5945s, 1995.

34. Morel, A., Darmon, M., and Delaage, M. Recognition of imidazole and histamine derivatives by monoclonal antibodies. Mol. Immunol., *27:* 995–1000, 1990.

35. Glennie, M. J., McBride, H. M., Worth, A. T., and Stevenson, G. T. Preparation and performance of bispecific F(ab′ γ)2 antibody containing thioether-linked Fab′ γ fragments. J. Immunol., *139:* 2367–2375, 1987.

36. Greenwood, F. C., and Hunter, W. M. The preparation of I-131 labeled human growth hormone of high specific radioactivity. Biochem. J., *89:* 114–123, 1963.

37. Goldenberg, D. M., and Hansen, H. J. Carcinoembryonic antigen present in human colonic neoplasms serially propagated in hamsters. Science (Wash. DC), *175:* 1117–1118, 1972.

38. Sharkey, R. M., Primus, F. J., and Goldenberg, D. M. Antibody protein dose and radioimmunodetection of GW-39 human colon tumor xenografts. Int. J. Cancer, *39:* 611–617, 1987.

39. Blumenthal, R. D., Fand, I., Sharkey, R. M., Boerman, O. C., Kashi, R., and Goldenberg, D. M. The effect of antibody protein dose on the uniformity of tumor distribution of radioantibodies: an autoradiographic study. Cancer Immunol. Immunother., *33:* 351–358, 1991.

40. Boerman, O. C., Sharkey, R. M., Wong, G. Y., Blumenthal, R. D., Aninipot, R. L., and Goldenberg, D. M. Influence of antibody protein dose on therapeutic efficacy of radioiodinated antibodies in nude mice bearing GW-39 human tumor. Cancer Immunol. Immunother., *35:* 127–134, 1992.

41. Karacay, H., Sharkey, R. M., McBride, W. J., Griffiths, G. L., Qu, Z., Chang, K., Hansen, H. J., and Goldenberg, D. M. Pretargeting for cancer radioimmunotherapy with bispecific antibodies: role of the bispecific antibody's valency for the tumor target antigen. Bioconjugate Chem., *13:* 1054–1070, 2002.

42. Siegel, J. A., Pawlyk, D. A., Lee, R. E., Sharkey, R. M., Horowitz, J., and Goldenberg, D. M. Tumor, red marrow, and organ dosimetry for $^{131}$I-labeled anti-carcinoembryonic antigen monoclonal antibody. Cancer Res., *50* (Suppl.)*:* 1039s–1042s, 1990.

43. Moshakis, V., McIlhinney, R. A. J., Raghaven, D., and Neville, A. M. Localization of human tumour xenografts after i.v. administration of radiolabelled monoclonal antibodies. Br. J. Cancer, *44:* 91–99, 1981.

44. Buchegger, F., Haskell, C. M., Schreyer, M., Scazziga, B. R., Randin, S., Carrel, S., and Mach, J. P. Radiolabeled fragments of monoclonal antibodies against carcinoembryonic antigen for localization of human colon carcinoma grafted into nude mice. J. Exp. Med., *158:* 413–427, 1983.

45. Sharkey, R. M., Blumenthal, R. D., Hansen, H. J., and Goldenberg, D. M. Biological considerations for radioimmunotherapy. Cancer Res., *50* (Suppl.)*:* 964s–969s, 1990.

46. Sharkey, R. M., Gold, D. V., Aninipot, R., Vagg, R., Ballance, C., Newman, E., Ostella, F., Hansen, H. J., and Goldenberg, D. M. Comparison of tumor targeting in nude mice murine monoclonal antibodies directed against different human colorectal cancer antigens. Cancer Res., *50* (Suppl.)*:* 828s–834s, 1990.

47. Behr, T. M., Blumenthal, R. D., Memtsoudis, S., Sharkey, R. M., Gratz, S., Becker, W., and Goldenberg, D. M. Cure of metastatic human colonic cancer in mice with radiolabeled monoclonal antibody fragments. Clin. Cancer Res., *6:* 4900–4907, 2000.

48. Behr, T. M., Behe, M., and Sgouros, G. Correlation of red marrow radiation dosimetry with myelotoxicity: empirical factors influencing the radiation-induced myelotoxicity of radiolabeled antibodies, fragments and peptides in pre-clinical and clinical settings. Cancer Biother. Radiopharm., *17:* 445–464, 2002.

49. Rossi, E. A., Sharkey, R. M., McBride, W., Karacay, H., Zeng, L., Hansen, H. J., Goldenberg, D. M., and Chang, C-H. Development of multivalent bispecific agents for pretargeting tumor localization and therapy. Clin. Cancer Res., *9* (Suppl.)*:* 3886s–3896s, 2003.